

BIFURCATION OF SPIKE EQUILIBRIA IN THE NEAR-SHADOW GIERER-MEINHARDT MODEL

THEODORE KOLOKOLNIKOV AND MICHAEL J. WARD

Department of Mathematics
University of British Columbia, Vancouver, Canada V6T 1Z2

(Communicated by Bjorn Sandstede)

ABSTRACT. In the limit of small activator diffusivity ε , and in a bounded domain in \mathbb{R}^N with $N = 1$ or $N = 2$ under homogeneous Neumann boundary conditions, the bifurcation behavior of an equilibrium one-spike solution to the Gierer-Meinhardt activator-inhibitor system is analyzed for different ranges of the inhibitor diffusivity D . When $D = \infty$, it is well-known that a one-spike solution for the resulting shadow Gierer-Meinhardt system is unstable, and the locations of unstable equilibria coincide with the points in the domain that are furthest away from the boundary. For a unit disk domain it is shown that as D is decreased below a critical bifurcation value D_c , with $D_c = O(\varepsilon^2 e^{2/\varepsilon})$, the spike at the origin becomes stable, and unstable spike solutions bifurcate from the origin. The locations of these bifurcating spikes tend to the boundary of the domain as D is decreased further. Similar bifurcation behavior is studied in a one-parameter family of dumbbell-shaped domains. This motivates a further analysis of the existence of certain near-boundary spikes. Their location and stability is given in terms of the modified Green's function. Finally, for the dumbbell-shaped domain, an intricate bifurcation structure is observed numerically as D is decreased below some $O(1)$ critical value.

1. Introduction. In the limit of small activator diffusivity, the bifurcation behavior of an equilibrium one-spike solution to the Gierer-Meinhardt activator-inhibitor system is analyzed, for different ranges of the inhibitor diffusivity D , in a bounded domain $\Omega \in \mathbb{R}^N$, with $N = 1$ or $N = 2$. The Gierer-Meinhardt model introduced in [8], and used to model various localization processes including biological morphogenesis and sea-shell patterns (cf. [11], [17], [18]), can be written in dimensionless form as (cf. [12])

$$a_t = \varepsilon^2 \Delta a - a + \frac{a^p}{h^q}, \quad x \in \Omega, \quad t > 0, \quad (1.1a)$$

$$\tau h_t = D \Delta h - h + \varepsilon^{-N} \frac{a^m}{h^s}, \quad x \in \Omega, \quad t > 0, \quad (1.1b)$$

$$\partial_n a = \partial_n h = 0, \quad x \in \partial\Omega. \quad (1.1c)$$

Here a and h represent the activator and the inhibitor concentrations, $\varepsilon^2 \ll 1$ and $D \gg O(\varepsilon^2)$ represent the diffusivity of the activator and inhibitor, τ is the inhibitor time constant, ∂_n denotes the outward normal derivative, and the exponents

2000 *Mathematics Subject Classification.* 35K57, 34B27, 92C15.

Key words and phrases. Gierer-Meinhardt model, reaction-diffusion equations, Green's function, pattern formation.

(p, q, m, s) satisfy

$$p > 1, \quad q > 0, \quad m > 0, \quad s \geq 0, \quad \frac{p-1}{q} < \frac{m}{s+1}. \quad (1.2)$$

In the limit $\varepsilon \rightarrow 0$, (1.1) admits spike solutions whereby the activator concentration a becomes localized near certain points on the boundary or in the interior of the domain Ω . Such solutions have been postulated to be responsible for a variety of localization processes in biological pattern formation, including the development of some sea shell patterns (cf. [17]). We will study the existence and stability of one-spike solutions to (1.1) when $\tau = 0$ in (1.1b).

When $\tau = 0$ and D is infinite, (1.1) reduces to the well-known nonlocal shadow system for the activator concentration a given by (cf. [12])

$$a_t = \varepsilon^2 \Delta a - a + \frac{a^p}{h^q}, \quad x \in \partial\Omega, \quad t > 0; \quad h = \left(\frac{\varepsilon^{-N}}{|\Omega|} \int_{\Omega} a^m dx \right)^{\frac{1}{s+1}}, \quad (1.3a)$$

$$\partial_n a = 0, \quad x \in \partial\Omega. \quad (1.3b)$$

Here $|\Omega|$ denotes the area of Ω . The steady-state and dynamical behavior of spike solutions to this shadow problem is now well-understood (see [3], [5], [9], [12], [16], [19], [22], [24], [25], [26], [27]). This problem admits both boundary spike solutions, which concentrate at critical points of the curvature of the boundary, and interior spike solutions, where the spikes are located strictly inside the domain. In this paper we only consider interior spike solutions. For $\varepsilon \rightarrow 0$, the equilibrium location of an interior one-spike solution to (1.1) is determined by critical points of the distance function (cf. [26]). Therefore, for a strictly convex domain in \mathbb{R}^2 , an equilibrium one-spike solution for this shadow problem is located asymptotically for $\varepsilon \rightarrow 0$ at the center of the largest circle that can be inscribed in the domain (cf. [22], [26]). For a dumbbell-shaped domain that is symmetric with respect to the x and y axes, such as that shown below in Fig. 4, an equilibrium one-spike solution is either located at the origin or in one of the two lobes of the dumbbell. These shadow spike solutions are stable with respect to the $O(1)$ eigenvalues in the spectrum of the linearization when the exponents satisfy (1.2) together with (cf. [24])

$$m = 2, \quad 1 < p \leq 1 + 4/N; \quad \text{or} \quad m = p + 1. \quad (1.4)$$

In this paper we assume that (1.4) holds. However, even under the condition (1.4), any interior one-spike solution to the shadow problem (1.1) is ultimately unstable, due to a positive but asymptotically exponentially small principal eigenvalue in the spectrum of the linearization (cf. [12], [24]). This eigenvalue is responsible for metastable behavior for the time-dependent problem.

In contrast, for (1.1) with $-\log \varepsilon \ll D \ll O(\varepsilon^2 e^{2d/\varepsilon})$, where d is the distance of the spike to the boundary, it was derived asymptotically in [15] that the equilibrium location x_0 of a one-spike solution to (1.1) is such that the gradient of the regular part R_m of the modified Green's function G_m for the Laplacian must vanish at x_0 .

This Green's function and its regular part satisfy

$$\Delta G_m = \frac{1}{|\Omega|} - \delta(x - x_0), \quad x \in \Omega, \quad (1.5a)$$

$$\partial_n G_m = 0, \quad x \in \partial\Omega; \quad \int_{\Omega} G_m dx = 0, \quad (1.5b)$$

$$R_m(x, x_0) = G_m(x, x_0) + \frac{1}{2\pi} \log|x - x_0|. \quad (1.5c)$$

The condition for a spike equilibrium is that $\nabla R_m = 0$ at $x = x_0$. By calculating an explicit formula for this gradient using complex analysis, and through many additional boundary integral numerical computations, it was conjectured in [15] that the location of an equilibrium one-spike solution to (1.1) in an arbitrary, possibly non-convex, simply-connected bounded domain is unique. If this conjecture holds, this solution must be stable since it necessarily corresponds to a minimum of R_m . This follows from [15] and [28], where it was shown that R_m tends to positive infinity near the boundary of a general domain Ω . The implication of this conjecture is that, for a dumbbell-shaped domain that is symmetric with respect to the x and y axes, there is a unique and stable one-spike solution located at the origin whenever D satisfies $-\log \varepsilon \ll D \ll O(\varepsilon^2 e^{2d/\varepsilon})$, where d is the distance of the spike to the boundary. However, as discussed in the previous paragraph, there can be three unstable equilibrium one-spike solutions for a dumbbell-shaped domain when $D = \infty$.

The main goal of this paper is to study this apparent paradox. Our analysis suggests that there is a bifurcation for one-spike solutions to (1.1) that occurs when D is exponentially large as $\varepsilon \rightarrow 0$. We give an explicit analysis of this bifurcation in the limit $\varepsilon \rightarrow 0$ for a one-dimensional slab domain, a circular cylindrical domain, and a one-parameter family of dumbbell-shaped domains. For a one-dimensional domain that contains an unstable one-spike equilibrium solution at the origin when $D = \infty$, it is shown that there is a critical bifurcation value D_c , with $D_c = O(\varepsilon^2 e^{2d/\varepsilon})$ where d is the distance of the spike to the boundary, such that as D decreases below D_c the spike at the midpoint of the domain becomes stable and unstable spike solutions bifurcate from this midpoint value. The locations of these bifurcating spikes tend to the boundary of the domain as D is decreased. A similar bifurcation scenario is found to occur for a circular cylindrical domain. Explicit asymptotic formulae for the bifurcation values D_c are calculated. A more intricate bifurcation behavior is analyzed for a one-parameter family of dumbbell-shaped domains. When $D = \infty$, an unstable spike for these domains can be located either in the neck or in one of the two lobes of the dumbbell. For $\varepsilon \rightarrow 0$, it is shown that the bifurcation behavior is such that when D is exponentially large, an equilibrium spike location in either lobe of the dumbbell will tend to the boundary of the domain. Moreover, as D decreases below some asymptotically exponentially large critical value, the spike in the neck of the dumbbell regains its stability as a result of a pitchfork bifurcation in the vertical direction. This critical value is calculated explicitly. These bifurcations are schematically illustrated in Fig. 1(a,b,c).

An additional bifurcation of equilibrium one-spike solutions for (1.1) in a dumbbell-shaped domain was found in [15] to occur when the inhibitor diffusivity D is on the range $O(\varepsilon^2) \ll D \ll O(-\log \varepsilon)$. On this range, the location of a one-spike solution to (1.1) is determined by the vanishing of the gradient of the regular part R of the

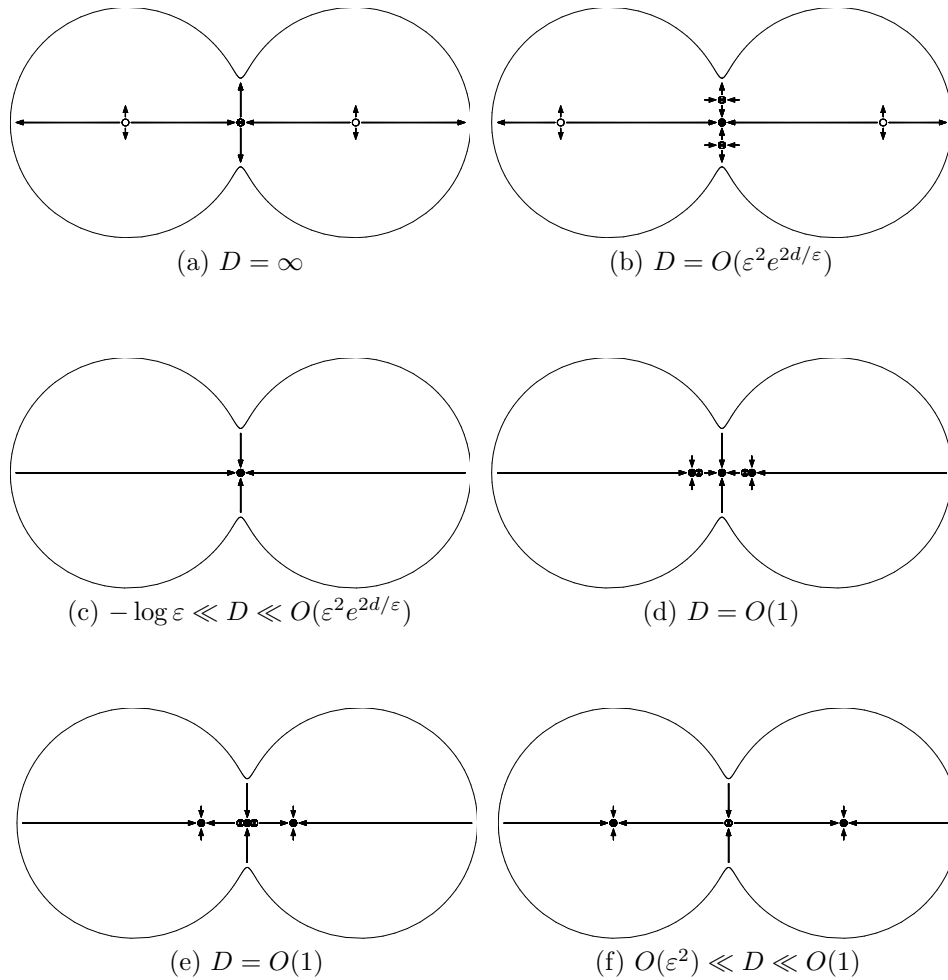


FIGURE 1. Schematic representations of vector fields and the bifurcations that occur for interior spike solutions in a dumbbell-shaped domain as D is decreased from ∞ to $O(\varepsilon^2)$. Stable equilibria, saddle points, and unstable equilibria correspond to black dots, hatched dots, and white dots, respectively. (a) For the shadow system all equilibria are unstable and correspond to critical points of the distance function from the center of the spike to the boundary. (b) In the intermediate regime, a competition between ∇R_m and the distance function determines the locations of an equilibrium interior spike. (c) For D large, but not exponentially large, there is a unique (stable) spike equilibrium inside the domain located where $\nabla R_m = 0$. (d) For $D = O(1)$ and $O(\varepsilon^2) \ll D \ll O(1)$, an interior spike is located where $\nabla R = 0$. (e) An intricate bifurcation structure may be present in the intermediate regime between (c) and (f). (f) On the range $O(\varepsilon^2) \ll D \ll O(1)$, R can be approximated by the distance function. Thus, in (f) the equilibria are the same as in (a), except that the spikes in the lobe of the dumbbell are stable and the direction field is reversed from (a).

reduced wave Green's function G , satisfying

$$\Delta G - \lambda^2 G = -\delta(x - x_0), \quad x \in \Omega, \quad (1.6a)$$

$$\partial_n G = 0, \quad x \in \partial\Omega, \quad (1.6b)$$

$$R(x, x_0) = G(x, x_0) + \frac{1}{2\pi} \log|x - x_0|. \quad (1.6c)$$

Here $\lambda^2 = 1/D$. For $D \ll 1$, it was shown in [15] that R is determined by the distance function. Therefore, for a dumbbell-shaped domain, there exists one-spike solutions to (1.1) in either the neck or the lobes of the dumbbell (see Fig. 1(f)). When $D \ll 1$, the spike solutions in the lobes of the dumbbell are stable since they correspond to local minima of R (cf. [15]). Similarly, for $D \ll 1$, the spike in the neck region is unstable since it corresponds to a saddle point of R . To reconcile this behavior for $D \ll 1$ with the conjectured uniqueness of a one-spike solution to (1.1) on the range $-\log \varepsilon \ll D \ll O(\varepsilon^2 e^{2d/\varepsilon})$, it was shown numerically for a certain dumbbell-shaped domain in [15] that there is a pitchfork bifurcation as D decreases below some $O(1)$ critical value. The effect of this bifurcation is that the spike in the neck of the dumbbell loses its stability to spike solutions that tend to the lobes of the dumbbell as D is decreased.

The second goal of this paper is to study numerically this additional pitchfork bifurcation behavior that occurs on the range $O(\varepsilon^2) \ll D \ll O(-\log \varepsilon)$ for a one-parameter family of dumbbell-shaped domains. Our numerical computations reveal the new result that this bifurcation can be either locally subcritical or supercritical. These bifurcation diagrams are obtained through boundary integral numerical computations of the zeroes of the gradient of the regular part R in (1.6c) evaluated at $x = x_0$. The relationship of the local behavior near the bifurcation point to the geometry of the neck region of the dumbbell-shaped domain is discussed.

In Fig. 1 we give a visual illustration of the various bifurcations that can occur for a one-spike solution to (1.1) in a dumbbell-shaped domain as D is decreased from infinity. The value of D decreases from Fig. 1(a) to Fig. 1(f). Pitchfork bifurcations at $x_0 = 0$ occur when D is exponentially large and again when $D = O(1)$. These bifurcations change the stability of the equilibrium spike at the origin. The bifurcation that occurs when $D = O(1)$ can be either subcritical or supercritical in D . In the lobes of the dumbbell, there are unstable spikes when $D = \infty$, and stable spikes when $O(\varepsilon^2) \ll D \ll O(1)$. In Fig. 1 we have only depicted the locations of interior spikes, defined as those for which the distance σ of the spike to the boundary $\partial\Omega$ is not asymptotically small.

Finally, we show that it is possible for spike equilibria to be located at certain points near the boundary of the domain, where the distance σ from the spike to the boundary satisfies $\varepsilon \ll \sigma \ll 1$. We show that such equilibria exist when $D = O(\varepsilon^q e^{2\sigma/\varepsilon})$, and that they are always unstable with respect to the direction perpendicular to the boundary. For a circle, these equilibria may occur near any boundary point because of the radial symmetry. The situation is more complicated for an arbitrary shaped domain. Using the explicit formula for the regular part of the Green's function for the class of dumbbell-shaped domains as shown in Fig. 1, we show that the near-boundary equilibria may occur only on the x or y -axis. Moreover, such equilibria along the x -axis are found to be unstable with respect to the tangential direction to the boundary, whereas those equilibria along the y -axis are stable in the tangential direction. Further work is needed to explore the relationship between these near-boundary spikes and spikes that are located on the

boundary. The behavior of boundary spikes should be determined by the curvature of the boundary and the local behavior of the gradient of the regular part of the modified Green's function on the boundary. This local behavior of the modified Green's function is computed explicitly for a dumbbell-shaped domain.

In our analysis we only consider bifurcations of equilibrium spike solutions. Other equilibrium solutions, such as ring solutions in a two-dimensional domain that concentrate as $\varepsilon \rightarrow 0$ on some circle of radius r_b are possible for reaction-diffusion systems when the inhibitor diffusivity D is either $D = O(1)$ or $D \ll O(1)$. These solutions have been found numerically for the Gray-Scott model (cf. [20], [21]) and can readily be constructed for the Gierer-Meinhardt model (1.1). However, ring solutions with ring radius $r_b = O(1)$ do not exist for (1.1) in the near-shadow limit where D is exponentially large. This is easily seen from the fact that the equilibrium ring radius must involve an asymptotic balance between the curvature of the ring and the diffusive flux of h in the core of the ring. Such a balance with $r_b = O(1)$ is not possible when D is exponentially large.

This paper is organized as follows. In §2 we outline the derivation of the equation of motion for a one-spike solution to (1.1) when D is exponentially large. This analysis, which relies heavily on the previous analyses in [15] and [12], is sketched for both a one and a two-dimensional domain. In §2, the bifurcation behavior of equilibrium spike solutions is studied in a one-dimensional domain. In §3 and §4 we analyze the pitchfork bifurcation behavior of an equilibrium one-spike solution in a circular cylindrical domain and in a one-parameter family of dumbbell-shaped domains, respectively. In §5 we study near-boundary spikes. In §6, we show numerically for the class of dumbbell-shaped domains of §4 that there is another pitchfork bifurcation point as D is decreased below some $O(1)$ critical value. The results of §4 and §6 can be depicted qualitatively as in Fig. 1. In §7 we formulate explicit conjectures, based on our asymptotic and numerical analyses, that await a rigorous proof.

2. The Dynamics of a Spike for Exponentially Large D . For $\tau = 0$ in (1.1b), we outline the derivation of the equation of motion for a spike solution to (1.1) in $\Omega \in \mathbb{R}^N$, when $N = 1$ and $N = 2$. For the shadow problem where $D = \infty$, the spike is metastable and the motion is determined by the exponentially weak interaction between the far-field behavior of the spike and the boundary $\partial\Omega$ (cf. [12]). For $D \gg 1$, but with D not exponentially large as $\varepsilon \rightarrow 0$, the exponentially weak interaction of the spike with the boundary is insignificant in comparison to the local behavior of the inhibitor field near $x = x_0$, which is determined by the Green's function G_m of (1.5) (cf. [15]). When D is exponentially large, the dynamics of x_0 is determined by a competition between the exponentially weak interaction of the spike with the boundary and the gradient of the regular part of the Green's function of (1.5). Since this competition is essentially a superposition of the previous results in ([12]) and ([15]), we only outline the key steps in the derivation of the dynamics for x_0 .

2.1. The One-Dimensional Case. Let $\Omega = [-1, 1]$, and suppose that the spike is located at $x = x_0 \in (-1, 1)$. For $D \gg 1$, we get from (1.1) that $h \sim \mathcal{H}$ on $x \in [-1, 1]$, and

$$a \sim \mathcal{H}^\gamma w [\varepsilon^{-1}(x - x_0)] , \quad \gamma \equiv \frac{q}{p-1} . \quad (2.1)$$

Here \mathcal{H} is a constant to be found, and $w(y)$ satisfies

$$w'' - w + w^p = 0, \quad -\infty < y < \infty, \tag{2.2a}$$

$$w(0) > 0, \quad w'(0) = 0; \quad w(y) \sim \alpha e^{-|y|}, \quad \text{as } y \rightarrow \pm\infty, \tag{2.2b}$$

for some $\alpha > 0$. Substituting (2.1) and the expansion $h = \mathcal{H} + h_1/D + \dots$ into (1.1b), we find that h_1 satisfies

$$h_{1xx} = \mathcal{H} - b_m \mathcal{H}^{\gamma m - s} \delta(x - x_0), \quad -1 < x < 1; \quad h_{1x}(\pm 1) = 0, \tag{2.3}$$

where $b_m \equiv \int_{-\infty}^{\infty} w^m dy$. This problem has a solution only when \mathcal{H} satisfies $\mathcal{H}^{\gamma m - (s+1)} = 2/b_m$. The solution for h_1 is

$$h_1 = 2\mathcal{H}G_m(x, x_0), \tag{2.4}$$

where G_m is the solution to (1.5a) and (1.5b) for $\Omega = [-1, 1]$. We calculate explicitly that

$$G_m(x, x_0) = \frac{1}{4}(x^2 + x_0^2) - \frac{1}{2}|x - x_0| + \frac{1}{6}. \tag{2.5}$$

To determine an equation of motion for x_0 , we substitute $a = \mathcal{H}^\gamma w(y) + v$ and $h = \mathcal{H} + h_1/D + \dots$ into (1.1a), where $y = \varepsilon^{-1}[x - x_0(t)]$. Assuming that $v \ll 1$, we then obtain the following quasi steady-state problem for v :

$$L_\varepsilon v \equiv \varepsilon^2 v_{xx} - v + pw^{p-1}v = \frac{2q\mathcal{H}^\gamma}{D} w^p G_m - \varepsilon^{-1} x'_0 \mathcal{H}^\gamma w', \quad -1 < x < 1, \tag{2.6a}$$

$$v_x = -\mathcal{H}^\gamma w_x, \quad x = \pm 1. \tag{2.6b}$$

As shown in [12], the eigenvalue problem $L_\varepsilon \phi = \lambda_0 \phi$ with $\phi_x(\pm 1) = 0$ has an exponentially small eigenvalue λ_0 , and the corresponding eigenfunction has the boundary layer form

$$\phi_0 \sim w' [\varepsilon^{-1}(x - x_0)] + \alpha e^{-\varepsilon^{-1}(1+x_0)} e^{-\varepsilon^{-1}(1+x)} - \alpha e^{-\varepsilon^{-1}(1-x_0)} e^{-\varepsilon^{-1}(1-x)}. \tag{2.7}$$

Multiplying (2.6a) by ϕ_0 , and integrating over $-1 < x < 1$, we let $\varepsilon \rightarrow 0$ to get the limiting solvability condition

$$\varepsilon^{-1} x'_0 \int_{-1}^1 (w')^2 dx = \frac{2q}{D} \int_{-1}^1 w' w^p G_m dx + \varepsilon^2 \phi_0 w_x|_{x=-1}^1. \tag{2.8}$$

Since w is localized near $x = x_0$, we let $y = \varepsilon^{-1}(x - x_0)$ in (2.8) to get

$$2x'_0 \beta = \frac{2\varepsilon q}{D(p+1)} \int_{-\infty}^{\infty} [w^{p+1}(y)]' G_m(x_0 + \varepsilon y, x_0) dy + \varepsilon^2 \phi_0 w_x|_{x=-1}^1, \tag{2.9}$$

where $\beta \equiv \int_0^\infty [w'(y)]^2 dy$. The second term on the right hand side in (2.9) can be calculated using (2.7) and the far-field behavior of (2.2b). The integral term on the right-hand side of (2.9) can be calculated by expanding G_m in one-sided limits near $x = x_0$, and integrating the resulting expression by parts. This yields,

$$x'_0 \sim \frac{\varepsilon \alpha^2}{\beta} \left(e^{-2\varepsilon^{-1}(1-x_0)} - e^{-2\varepsilon^{-1}(1+x_0)} \right) - \frac{2\varepsilon^2 q}{D(p+1)} \left[\frac{G_{mx}(x_0^+, x_0) + G_{mx}(x_0^-, x_0)}{2} \right] \left(\frac{\int_0^\infty [w(y)]^{p+1} dy}{\int_0^\infty [w'(y)]^2 dy} \right). \tag{2.10}$$

Using (2.2) we can calculate the ratio of the two integrals on the right-hand side of (2.10). In addition, we can use (2.5) to calculate G_m in (2.10). This yields,

$$\frac{\int_0^\infty [w(y)]^{p+1} dy}{\int_0^\infty [w'(y)]^2 dy} = 2 \left(\frac{p+1}{p-1} \right), \quad G_{mx}(x_0^+, x_0) + G_{mx}(x_0^-, x_0) = x_0. \quad (2.11)$$

Substituting (2.11) into (2.10), we obtain the following result:

Proposition 2.1: Let $\varepsilon \ll 1$, $\Omega = [-1, 1]$, and assume that $x_0 \in (-1, 1)$ with $1 - x_0 \gg O(\varepsilon)$ and $1 + x_0 \gg O(\varepsilon)$. Then, for D exponentially large as $\varepsilon \rightarrow 0$, the spike location x_0 satisfies the differential equation

$$\begin{aligned} \frac{dx_0}{dt} &\sim H(x_0) \equiv \frac{\varepsilon \alpha^2}{\beta} \left(e^{-2\varepsilon^{-1}(1-x_0)} - e^{-2\varepsilon^{-1}(1+x_0)} \right) - \frac{2\varepsilon^2 q}{D(p-1)} x_0, \\ \beta &\equiv \int_0^\infty [w'(y)]^2 dy. \end{aligned} \quad (2.12)$$

Here α is defined in (2.2b).

For any D , (2.12) has an equilibrium at $x_0 = 0$. This solution is stable if $H'(0) < 0$, and is unstable when $H'(0) > 0$. Setting $H'(0) = 0$, we obtain the bifurcation value $D \sim D_c$, where

$$D_c = \frac{\varepsilon^2 q \beta}{2\alpha^2(p-1)} e^{2/\varepsilon}. \quad (2.13)$$

This critical value, which is exponentially large as $\varepsilon \rightarrow 0$, was calculated in [14]. The next result is obtained by writing (2.12) in terms of D_c .

Proposition 2.2: Under the conditions of proposition 2.1, $x_0(t)$ satisfies

$$\frac{dx_0}{dt} \sim \frac{4\varepsilon \alpha^2}{\beta} \left(\frac{\varepsilon \sinh(2x_0/\varepsilon)}{2x_0} - \frac{D_c}{D} \right) e^{-2/\varepsilon} x_0. \quad (2.14)$$

Here D_c is defined in (2.13). The spike location at $x_0 = 0$ is stable when $D < D_c$ and is unstable when $D > D_c$. When $D < D_c$, (2.14) has two unstable equilibria, which are the roots of

$$\frac{2y}{\sinh(2y)} = \frac{D}{D_c}, \quad y \equiv x_0/\varepsilon. \quad (2.15)$$

This critical value D_c depends on α and β defined by (2.2b) and (2.12), respectively. By calculating the solution w to (2.2), we can obtain numerical values for these quantities as

$$\alpha = [2(p+1)]^{1/(p-1)} \quad p > 1; \quad (2.16a)$$

$$\beta = 3/5, \quad p = 2; \quad \beta = 2/3, \quad p = 3; \quad \beta = 0.681, \quad p = 4. \quad (2.16b)$$

As a remark, we can determine β without pointwise values of $w(y)$. A simple calculation shows that

$$\beta = \int_0^{w_m} \left[(w^2 - w_m^2) - \frac{2}{p+1} (w^{p+1} - w_m^{p+1}) \right]^{1/2} dw, \quad w_m = \left(\frac{p+1}{2} \right)^{1/(p-1)}. \quad (2.16c)$$

In Fig. 2 we plot the bifurcation diagram $y \geq 0$ as a function of D/D_c from (2.15). Qualitatively, (2.15) shows that the ratio D/D_c decreases as $x_0 > 0$ increases. Therefore, the unstable spikes, which bifurcate symmetrically from $x_0 = 0$ at the value $D = D_c$, move towards the endpoints of the domain as D decreases below D_c .

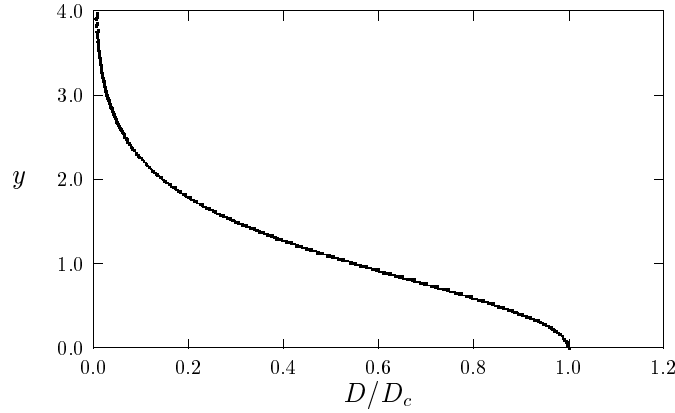


FIGURE 2. Plot of the local bifurcation diagram (2.15) where $y = 2x_0/\varepsilon$.

Since our analysis has only considered interior spike solutions, we cannot describe the process by which an unstable interior spike merges onto the boundary of Ω at some further critical value of D .

2.2. The Two-Dimensional Case. Next, we assume that $\Omega \in \mathbb{R}^2$, and that $\partial\Omega$ is smooth. Let $x_0 \in \Omega$, with $\text{dist}(x_0; \partial\Omega) \gg O(\varepsilon)$. For $D \gg 1$, we get from (1.1) that $h \sim \mathcal{H}$ on Ω , and that

$$a \sim \mathcal{H}^\gamma w(\varepsilon^{-1}|x - x_0|), \quad \gamma \equiv \frac{q}{p-1}. \tag{2.17}$$

Here the radially symmetric solution $w(\rho)$, with $\rho \equiv |y|$, satisfies

$$w'' + \frac{1}{\rho}w' - w + w^p = 0, \quad \rho \geq 0, \tag{2.18a}$$

$$w(0) > 0, \quad w'(0) = 0; \quad w(\rho) \sim \alpha\rho^{-1/2}e^{-\rho}, \quad \text{as } \rho \rightarrow \infty, \tag{2.18b}$$

for some $\alpha > 0$. Substituting (2.17) and the expansion $h = \mathcal{H} + h_1/D + \dots$ into (1.1b), we find that h_1 satisfies

$$\Delta h_1 = \mathcal{H} - b_m \mathcal{H}^{\gamma m - s} \delta(x - x_0), \quad x \in \Omega; \quad \partial_n h = 0, \quad x \in \partial\Omega, \tag{2.19}$$

where $b_m \equiv \int_{\mathbb{R}^2} w^m dy$. This problem has a solution only when \mathcal{H} satisfies $\mathcal{H}^{\gamma m - (s+1)} = |\Omega|/b_m$, where $|\Omega|$ is the area of Ω . The solution for h_1 is $h_1 = \mathcal{H}|\Omega|G_m$, where G_m satisfies (1.5).

To determine an equation of motion for x_0 , we substitute $a = \mathcal{H}^\gamma w(y) + v$ and $h = \mathcal{H} + h_1/D + \dots$ into (1.1a), where $y = \varepsilon^{-1}[x - x_0(t)]$. Assuming that $v \ll 1$, we then obtain, in place of (2.6), the following quasi steady-state problem for v :

$$L_\varepsilon v \equiv \varepsilon^2 \Delta v - v + pw^{p-1}v = \frac{q|\Omega|\mathcal{H}^\gamma}{D} w^p G_m - \varepsilon^{-1} \frac{(x - x_0)}{|x - x_0|} \cdot x'_0 \mathcal{H}^\gamma w', \quad x \in \Omega, \tag{2.20a}$$

$$\partial_n v = -\mathcal{H}^\gamma \partial_n w, \quad x \in \partial\Omega. \tag{2.20b}$$

As shown in [12], the eigenvalue problem $L_\varepsilon \phi = \lambda_0 \phi$ in Ω , together with $\partial_n \phi = 0$ on $\partial\Omega$, has two exponentially small eigenvalues λ_i , with $i = 1, 2$. The corresponding eigenfunctions have the boundary layer form

$$\phi_i \sim \partial_{x_i} w + \hat{\phi}_i. \tag{2.21}$$

Here $x = (x_1, x_2)$, and $\hat{\phi}_i$ is a boundary layer function localized near $\partial\Omega$ that allows the no-flux condition for ϕ_i on $\partial\Omega$ to be satisfied. Multiplying (2.20a) by ϕ_i , and integrating over Ω , we let $\varepsilon \rightarrow 0$ to get the limiting solvability condition

$$\varepsilon^{-1} x'_0 \cdot \int_{\Omega} \frac{(x - x_0)}{|x - x_0|} w' \partial_{x_i} w \, dx = \frac{q|\Omega|}{D} \int_{\Omega} G_m w^p \partial_{x_i} w \, dx + \int_{\partial\Omega} \varepsilon^2 \phi_i \partial_n w \, dS, \tag{2.22}$$

for $i = 1, 2$. Since w is localized near $x = x_0$, we let $y = \varepsilon^{-1}(x - x_0)$ in (2.22), and use the following local behavior for G_m obtained from (1.5c):

$$G_m(x_0 + \varepsilon y, x_0) = -\frac{1}{2\pi} \log(\varepsilon|y|) + R_m(x_0, x_0) + \varepsilon y \cdot \nabla R_{m0} + O(|y|^2). \tag{2.23}$$

Here $\nabla R_{m0} \equiv \nabla R_m|_{x=x_0}$. In this way, we obtain from (2.22) that

$$x'_0 \cdot \int_{\mathbb{R}^2} \frac{yy_i}{|y|^2} \left[w'(|y|) \right]^2 \, dy = \frac{\varepsilon^2 q |\Omega|}{D(p+1)} \nabla R_{m0} \cdot \int_{\mathbb{R}^2} \frac{yy_i}{|y|} \left[w^{p+1}(y) \right]' \, dy + \int_{\partial\Omega} \varepsilon^2 \phi_i \partial_n w \, dS, \tag{2.24}$$

for $i = 1, 2$, where $y = (y_1, y_2)$. The integrals over \mathbb{R}^2 in (2.24) were calculated in [15] (see equations (2.43) and (2.45) of [15]). The integral in (2.24) over $\partial\Omega$ was calculated in [12] (see §3.3 of [12]). In this way, we obtain the following main result:

Proposition 2.3: Let $\varepsilon \ll 1$, and assume that $x_0 \in \Omega$ with $\text{dist}(x_0; \partial\Omega) \gg O(\varepsilon)$. Then, for D exponentially large as $\varepsilon \rightarrow 0$, the spike location x_0 satisfies the differential equation

$$\frac{dx_0}{dt} \sim \frac{2\varepsilon q}{p-1} \left[\frac{\alpha^2}{2\pi\beta} \left(\frac{p-1}{q} \right) J - \frac{\varepsilon|\Omega|}{D} \nabla R_{m0} \right], \tag{2.25a}$$

where the vector boundary integral J is defined by

$$J = \int_{\partial\Omega} \frac{\hat{r}}{r} e^{-2r/\varepsilon} (1 + \hat{r} \cdot \hat{n}) \hat{r} \cdot \hat{n} \, dS. \tag{2.25b}$$

Here $r = |x - x_0|$, and $\hat{r} = (x - x_0)/r$. The constant β in (2.25a) is defined by

$$\beta \equiv \int_0^\infty \rho \left[w'(\rho) \right]^2 \, d\rho. \tag{2.26}$$

The dynamics (2.25) for x_0 expresses a competition between ∇R_{m0} , inherited from the local inhibitor field, and the boundary integral J , representing the exponentially weak interaction between the tail of the spike and the boundary $\partial\Omega$. The dynamics depends on the constants α and β , defined in (2.18b) and (2.26). For several values of p , these constants were computed numerically in [22], with the result

$$\begin{aligned} \alpha &= 10.80, & \beta &= 2.47, & p &= 2; \\ \alpha &= 3.50, & \beta &= 1.86, & p &= 3; \\ \alpha &= 2.12, & \beta &= 1.50, & p &= 4. \end{aligned} \tag{2.27}$$

In §3 and §4 we examine some special cases of (2.25).

When $D \gg 1$, but with D not exponentially large as $\varepsilon \rightarrow 0$, (2.25) reduces to the gradient flow

$$\frac{dx_0}{dt} \sim -\frac{2\varepsilon^2 q |\Omega|}{D(p-1)} \nabla R_{m0}. \tag{2.28}$$

This limiting result was derived independently in [23] and [6]. The conjecture of [15] is that $\nabla R_{m0} = 0$ has exactly one root in the interior of an arbitrary, possibly non-convex, bounded and simply-connected domain Ω .

3. A Radially Symmetric Domain: D Exponentially Large. In this section we analyze the dynamics and equilibria of a spike solution to (1.1) in a circular cylindrical domain Ω of radius one when D is exponentially large. The bifurcation behavior of the spike equilibria is found to be qualitatively similar to the analysis in §2.1 for the one-dimensional slab geometry.

We look for a solution to (1.1) that has an interior spike centered at $x_0 \in \Omega$. Since $|\Omega| = \pi$, we obtain from (2.25) that the dynamics of the spike satisfies

$$\frac{dx_0}{dt} \sim \frac{2\varepsilon q}{p-1} \left[\frac{\alpha^2}{2\pi\beta} \left(\frac{p-1}{q} \right) J - \frac{\varepsilon\pi}{D} \nabla R_{m0} \right], \quad (3.1)$$

where J was defined in (2.25b), and the constants α and β were defined in (2.18b) and (2.26), respectively. For such a ball domain, the gradient of R_{m0} was calculated previously in [23] as

$$\nabla R_{m0} = \frac{1}{2\pi} \left(\frac{2 - |x_0|^2}{1 - |x_0|^2} \right) x_0. \quad (3.2)$$

By symmetry, we need only look for an equilibrium solution to (3.1) on the segment $x_0 \in [0, 1)$ of the positive real axis. To do so, we need Laplace's formula (cf. [29]) valid for $\varepsilon \ll 1$,

$$\int_{\partial\Omega} r^{-1} F(r) e^{-2r/\varepsilon} dS \sim \sum \left(\frac{\pi\varepsilon}{r_m} \right)^{1/2} F(r_m) (1 - \kappa_m r_m)^{-1/2} e^{-2r_m/\varepsilon}. \quad (3.3a)$$

Comparing (2.25b) with (3.3a), we take

$$F(r) \equiv \hat{r} (1 + \hat{r} \cdot \hat{n}) \hat{r} \cdot \hat{n}. \quad (3.3b)$$

In (3.3a), $r_m = \text{dist}(x_0; \partial\Omega)$, κ_m is the curvature of $\partial\Omega$ at x_m , and the sum is taken over all $x_m \in \partial\Omega$ that are closest to x_0 . The sign convention is such that $\kappa_m > 0$ if Ω is convex at x_m .

We first suppose that $x_0 \gg O(\varepsilon)$ and that $1 - x_0 \gg O(\varepsilon)$. In this case, the point $(1, 0)$ on $\partial\Omega$ is the unique point closest to x_0 . Using (3.3) with $\hat{r} = (1, 0)$, $\hat{n} = (1, 0)$, and $\kappa_m = 1$, we get for $\varepsilon \ll 1$ that

$$J \sim 2 \left(\frac{\pi\varepsilon}{x_0(1-x_0)} \right)^{1/2} e^{-2\varepsilon^{-1}(1-x_0)\hat{i}}, \quad (3.4)$$

where $\hat{i} = (1, 0)$.

Next, suppose that $x_0 > 0$ with $x_0 = O(\varepsilon)$. In this case, Laplace's formula (3.3) fails since the asymptotic contribution to J arises from the entire integral over the boundary rather than from a discrete set of points. Parameterizing $\partial\Omega$ by $x = \cos t$ and $y = \sin t$, we calculate for $x_0 \ll 1$ that

$$\begin{aligned} r &= 1 - x_0 \cos t + O(x_0^2); \\ \hat{r} &= (\cos t, \sin t) + x_0 (-\sin^2 t, \sin t \cos t) + O(x_0^2); \\ \hat{r} \cdot \hat{n} &= 1 + O(x_0^2). \end{aligned} \quad (3.5)$$

Substituting (3.5) into (2.25b), we obtain to leading order that

$$J \sim 2\hat{i} e^{-2/\varepsilon} \int_0^{2\pi} (\cos t) e^{2\varepsilon^{-1}x_0 \cos t} dt. \quad (3.6)$$

Since the modified Bessel function I_1 of the first kind of order one has the integral representation (cf. [1]),

$$I_1(x) = \frac{1}{2\pi} \int_0^{2\pi} (\cos \theta) e^{x \cos \theta} d\theta, \tag{3.7}$$

we obtain that

$$J \sim 4\pi \hat{i} e^{-2/\varepsilon} I_1(2x_0/\varepsilon). \tag{3.8}$$

This expression is valid for $x_0 = O(\varepsilon)$. When $x_0 \ll O(\varepsilon)$, the asymptotic evaluation of J is obtained by using the local behavior $I_1(z) \sim z/2$ as $z \rightarrow 0$ in (3.8). This yields,

$$J \sim 4\pi \varepsilon^{-1} \hat{i} x_0 e^{-2/\varepsilon}. \tag{3.9}$$

Using $I_1(z) \sim (2\pi z)^{-1/2} e^z$ in (3.8), we obtain that the far-field form of (3.8) for $x_0 \gg O(\varepsilon)$ agrees with the leading order behavior of (3.4) as $x_0 \rightarrow 0$. Combining (3.4) and (3.8), we can write a uniformly valid leading order approximation to J as

$$J \sim \frac{4\pi \hat{i} e^{-2/\varepsilon}}{\sqrt{1-x_0}} I_1(2x_0/\varepsilon). \tag{3.10}$$

This formula is valid for $x_0 \geq 0$, with $1-x_0 \gg O(\varepsilon)$.

The origin $x_0 = 0$ is an equilibrium point for (3.1) for any $D > 0$. Using (3.9) and (3.2) we can write the local behavior for (3.1) when $x_0 \ll 1$ as

$$\frac{dx_0}{dt} \sim \frac{2\varepsilon^2 q}{(p-1)D} \left(\frac{D}{D_c} - 1 \right) x_0, \tag{3.11a}$$

where D_c is defined by

$$D_c = \frac{\varepsilon^2 q \beta}{2\alpha^2(p-1)} e^{2/\varepsilon}. \tag{3.11b}$$

This critical value has the same form as was calculated for the one-dimensional slab geometry in (2.13), except that the constants α and β depend on the dimension. Hence, the equilibrium $x_0 = 0$ is unstable when $D > D_c$, and is stable when $D < D_c$. The constants α and β in (3.11b) are given for various p in (2.27). Substituting (3.2) and (3.10) into (3.1), we obtain the following main result:

Proposition 3.1: *Let $\varepsilon \ll 1$ and assume that the spike location x_0 within the unit ball is along the segment of the real axis satisfying $x_0 \geq 0$ with $1-x_0 \gg O(\varepsilon)$. Then, the trajectory $x_0(t)$ of an interior spike solution satisfies*

$$\frac{dx_0}{dt} \sim \frac{2\varepsilon^2 q}{(p-1)D} \left[\frac{D}{D_c} - \frac{1}{H(x_0)} \right] \frac{\varepsilon I_1(2x_0/\varepsilon)}{\sqrt{1-x_0}}, \tag{3.12a}$$

where D_c is defined in (3.11b), and $H(x_0)$ is defined by

$$H(x_0) \equiv \frac{\varepsilon \sqrt{1-x_0}(1+x_0) I_1(2x_0/\varepsilon)}{x_0(1-x_0^2/2)}. \tag{3.12b}$$

Since $H(0) = 1$, the equilibrium location $x_0 = 0$ is stable when $D < D_c$ and is unstable when $D > D_c$. On the range $x_0 > 0$ with $1-x_0 \gg O(\varepsilon)$, for each $D < D_c$ there is a unique unstable equilibrium solution to (3.12a) satisfying

$$\frac{D_c}{D} = H(x_0). \tag{3.13}$$

The local behavior of the bifurcating branch, obtained by setting $y = x_0/\varepsilon$ in (3.13), is given by

$$\frac{D}{D_c} = \frac{y}{I_1(2y)}. \tag{3.14}$$

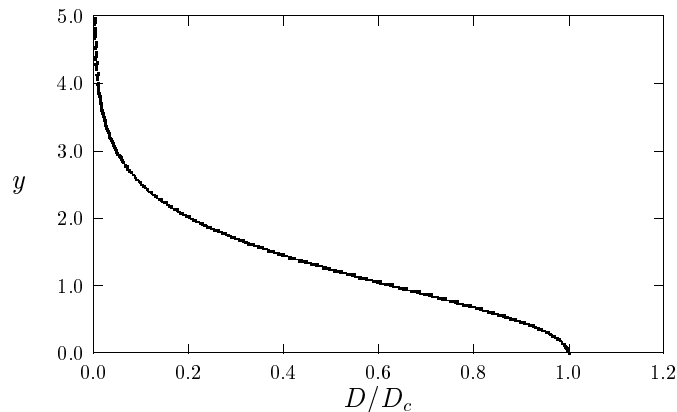


FIGURE 3. Plot of the local bifurcation diagram (3.14) where $y = x_0/\varepsilon$.

In Fig. 3 we plot the local bifurcation behavior (3.14). Notice that, although the bifurcation point D_c for the one-dimensional slab geometry and the unit ball are the same, the local bifurcation behaviors (3.14) and (2.15) for the ball and slab domains, respectively, are different when $x_0 = O(\varepsilon)$. However, for $y \ll 1$ (i.e. $x_0 \ll \varepsilon$), we can use $I_1(2y) \sim 2y$ and $\sinh(2y) \sim 2y$ in (3.14) and (2.15), respectively, to conclude that (3.14) and (2.15) are the same to leading order when $x_0 \ll \varepsilon$.

Qualitatively, we see that, except within an $O(\varepsilon)$ neighborhood of $x_0 = 1$ where (3.13) is not valid, (3.13) shows that the ratio D_c/D increases as x_0 increases. Therefore, the unstable spike, which bifurcated from $x_0 = 0$ at the value $D = D_c$, moves towards the boundary of the circle as D decreases below D_c . From (3.11b), the critical value D_c is exponentially large as $\varepsilon \rightarrow 0$ and depends on the parameters α and β given numerically in (2.27).

Since our analysis has only considered interior spike solutions that interact exponentially weakly with the boundary, we again cannot describe the process by which the unstable interior spike merges onto the boundary of the unit ball at some further critical value of D . However, using (3.13) we can give an estimate of the value of D for which a spike approaches to within an $O(\sigma)$ neighborhood of the boundary, where $\varepsilon \ll \sigma \ll 1$. Let $x_0 = 1 - \sigma$ in (3.13). A simple calculation using (3.11b), (3.12b), and the large argument expansion of $I_1(z)$, yields

$$D \sim \frac{\beta\sqrt{\pi}}{4\alpha^2} \left(\frac{q}{p-1} \right) \left(\frac{\varepsilon}{\sigma} \right)^{1/2} e^{2\sigma/\varepsilon}. \quad (3.15)$$

Since we have specified $x_0 \in (0, 1]$ at the outset of the analysis, our bifurcation analysis cannot determine the direction in which the equilibrium spike moves towards the boundary as D is decreased. This degeneracy in the fundamental problem can be broken by a slight perturbation in the shape of the domain. A resulting imperfection sensitivity analysis would presumably be able to resolve the degeneracy and determine a unique direction for the bifurcating spike.

4. A Dumbbell-Shaped Domain: D Exponentially Large. When D is exponentially large, we now analyze the dynamics and equilibria of a one-spike solution

to (1.1) with $\tau = 0$ in a one-parameter family of dumbbell-shaped domains. Let $z \in \mathcal{B}$, where \mathcal{B} is the unit circle, and define the complex mapping $w = f(z)$, with $z = u + iv$, by

$$w = f(z) = \frac{(1 - b^2)z}{z^2 - b^2}. \quad (4.1)$$

Here b is real and $b > 1$. The resulting domain $\Omega = f(\mathcal{B})$ is shown in Fig. 4 for several values of b . Notice that $\Omega \rightarrow \mathcal{B}$ as $b \rightarrow \infty$. Moreover, as $\delta \equiv b - 1 \rightarrow 0^+$, Ω approaches the union of two circles centered at $(\pm 1/2, 0)$, with radius $1/2$, that are connected by a thin neck region of width $2\delta + O(\delta^2)$. This class of dumbbell-shaped domains is symmetric with respect to both the x and y axes. Therefore, when $D = \infty$, and for a certain range of b , we expect that there will be three equilibrium one-spike solutions, one centered at the origin and the other two centered on the x -axis in the lobes of the dumbbell. As a remark, this class of domains was considered previously in [10], where it was shown that the regular part of the Green's function under Dirichlet boundary conditions has more than one minima when $b < \sqrt{3}$. It is easy to show that Ω is non-convex only when $1 < b < b_c \equiv 1 + \sqrt{2}$.

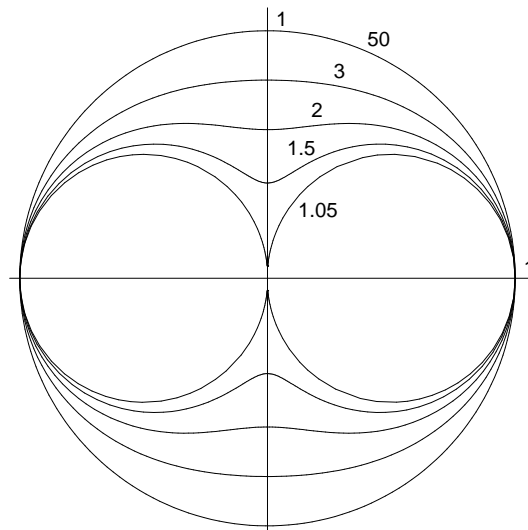


FIGURE 4. The boundary of $\Omega = f(\mathcal{B})$, with $f(z)$ as given in (4.1), for the values of b as shown.

Let x_0 be the location of a one-spike solution to (1.1) in Ω , with pre-image point $z_0 \in \mathcal{B}$ satisfying $x_0 = f(z_0)$. Let ∇R_{m0} denote the gradient of the regular part of the modified Green's function (1.5) at $x = x_0$. To give an explicit analysis of the equilibrium spike bifurcation behavior in Ω as D is decreased from infinity, we require an explicit formula for this gradient. In [15] (see Theorem 4.1 of [15]), a complex variable method was used to derive this formula for a general class of mappings of the unit disk. Applying this result to (4.1), we obtain

$$\nabla R_{m0} = \frac{\nabla s(z_0)}{f'(z_0)}, \quad (4.2a)$$

where

$$\nabla s(z_0) = \frac{1}{2\pi} \left(\frac{z_0}{1-|z_0|^2} - \frac{2b^2\bar{z}_0}{\bar{z}_0^4 - b^4} + \frac{b^2\bar{z}_0}{\bar{z}_0^2 b^2 - 1} - \frac{(b^4 - 1)^2 (|z_0|^2 - 1)(z_0 + b^2\bar{z}_0)(\bar{z}_0^2 + b^2)}{(b^4 + 1)(\bar{z}_0^2 b^2 - 1)(z_0^2 - b^2)(\bar{z}_0^2 - b^2)^2} \right), \quad (4.2b)$$

and

$$f'(z_0) = (b^2 - 1) \frac{(z_0^2 + b^2)}{(z_0^2 - b^2)^2}, \quad x_0 = f(z_0). \quad (4.2c)$$

In (4.2), we interpret vectors as complex numbers so that $\nabla R_{m0} = \partial_x R_{m0} + i\partial_y R_{m0}$. The area $|\Omega|$ of Ω , which is needed below, was derived in [15] to be

$$|\Omega| = \pi \frac{(b^4 + 1)}{(b^2 + 1)^2}. \quad (4.3)$$

Note that $|\Omega| \rightarrow \pi$ as $b \rightarrow \infty$, and $|\Omega| \rightarrow \pi/2$ as $b \rightarrow 1^+$, when Ω reduces to two circles each of radius $1/2$.

The dynamics and equilibria of a one-spike solution to (1.1) in Ω is obtained by substituting (4.2) and (4.3) into (2.25). We show below that the bifurcation behavior of equilibria to (2.25) is as sketched in Fig. 1(b). In §4.1 we analyze this behavior for the equilibrium spike located at the origin $(0, 0)$ in the neck region of the dumbbell. In §4.2 we analyze equilibrium spikes in the lobes of the dumbbell.

4.1. The Neck Region of the Dumbbell. When $D = \infty$, the equilibrium spike solution at the origin is unstable. However, as we show below, as D decreases below some critical value D_c this equilibrium solution regains its stability, and new unstable equilibria appear at the points $(0, \pm y_0)$ in Ω for some $y_0 > 0$. These equilibria move along the vertical axis towards the boundary $\partial\Omega$ as D is decreased below D_c (see Fig. 1(b)).

To analyze the spike behavior, we must calculate the integral J in (2.25) asymptotically. To do so, we parameterize $\partial\Omega$ by letting $z = e^{it}$, for $-\pi \leq t < \pi$, and $w(t) = f(e^{it}) = \xi(t) + i\eta(t)$. Using (4.1), we calculate

$$\xi(t) = \frac{(b^2 - 1)^2 \cos t}{b^4 + 1 - 2b^2 \cos 2t}, \quad \eta(t) = \frac{(b^4 - 1) \sin t}{b^4 + 1 - 2b^2 \cos 2t}. \quad (4.4)$$

For a spike located at $(0, y_0)$ in Ω , with $y_0 > 0$ but small, the dominant contribution to J arises from the points corresponding to $t = \pm\pi/2$, labelled by $(0, \pm y_m)$, where

$$y_m = \left(\frac{b^2 - 1}{b^2 + 1} \right). \quad (4.5)$$

A simple calculation using (4.4) shows that the curvature κ_m of $\partial\Omega$ at $(0, \pm y_m)$ is

$$\kappa_m = \frac{\xi' \eta'' - \eta' \xi''}{[\eta'^2 + \xi'^2]^{3/2}} \Big|_{t=\pm\pi/2} = \left(\frac{b^2 + 1}{b^2 - 1} \right)^3 \left[1 - \frac{8b^2}{(b^2 + 1)^2} \right]. \quad (4.6)$$

By symmetry, the vector integral J in (2.25) has the form $J = (0, J_2)$. When $y_0 \ll y_m - \varepsilon$, we evaluate the integral J asymptotically in (2.25) for $\varepsilon \rightarrow 0$, to obtain

$$J_2 \sim 2\sqrt{\pi\varepsilon} e^{-2y_m/\varepsilon} \left[\frac{e^{2y_0/\varepsilon}}{\sqrt{r_{m1}(1 - \kappa_m r_{m1})}} - \frac{e^{-2y_0/\varepsilon}}{\sqrt{r_{m2}(1 - \kappa_m r_{m2})}} \right], \quad (4.7a)$$

where

$$r_{m1} = y_m - y_0, \quad r_{m2} = y_m + y_0. \tag{4.7b}$$

When $|y_0| = O(\varepsilon)$, we calculate

$$J_2 \sim 4 \left(\frac{\pi\varepsilon}{y_m(1 - \kappa_m y_m)} \right)^{1/2} e^{-2y_m/\varepsilon} \sinh(2y_0/\varepsilon). \tag{4.8}$$

Next, we calculate ∇R_{m0} near the origin. Let $z_0 = iv_0 \in \mathcal{B}$, and $w_0 = iy_0 \in \Omega$. Since $w = f(z)$, we calculate that

$$v_0 = \frac{(b^2 - 1)}{2y_0} - \left[\left(\frac{b^2 - 1}{2y_0} \right)^2 - b^2 \right]^{1/2}, \tag{4.9a}$$

and

$$y_0 \sim f'(0)v_0, \quad \text{where} \quad f'(0) = \frac{(b^2 - 1)}{b^2}, \quad \text{as} \quad v_0 \rightarrow 0. \tag{4.9b}$$

Using (4.3) and (4.9b), we can calculate $|\Omega|\partial_y R_{m0}$ in (4.2) in terms of y_0 for $|y_0| \ll 1$. A simple, but lengthy, calculation yields that

$$|\Omega|\partial_y R_{m0} = y\mathcal{G}(b), \quad \mathcal{G}(b) = \frac{(b^2 - 1)}{2(b^4 - 1)^2} [2b^6 + 3b^4 + 2b^2 - 1]. \tag{4.10}$$

Substituting (4.8) and (4.10) into (2.25a), we obtain the following main result:

Proposition 4.1: *Let $\varepsilon \ll 1$ and assume that the spike location $(0, y_0)$ on the y -axis satisfies $y_0 = O(\varepsilon)$. Then, the local trajectory $y_0(t)$ satisfies*

$$\frac{dy_0}{dt} \sim \varepsilon^{1/2} \mu_0 e^{-2y_m/\varepsilon} \left[\frac{\sinh(2y_0/\varepsilon)}{(2y_0/\varepsilon)} - \frac{D_c}{D} \right] y_0, \tag{4.11a}$$

where D_c and μ_0 satisfy

$$D_c = \frac{\varepsilon^2 \beta}{4\alpha^2} \left(\frac{q}{p-1} \right) \left(\frac{\pi}{\varepsilon} \right)^{1/2} [y_m(1 - \kappa_m y_m)]^{1/2} \mathcal{G}(b) e^{2y_m/\varepsilon}, \tag{4.11b}$$

$$\mu_0 = \frac{8\alpha^2}{\sqrt{\pi}\beta} [y_m(1 - \kappa_m y_m)]^{-1/2}. \tag{4.11c}$$

When $D > D_c$, $y_0 = 0$ is the unique, and unstable, equilibrium solution for (4.11a). For $D < D_c$, $y_0 = 0$ is stable, and there are two unstable equilibria with $|y_0| = O(\varepsilon)$, satisfying

$$\frac{2\zeta}{\sinh(2\zeta)} = \frac{D}{D_c}, \quad \zeta = y_0/\varepsilon. \tag{4.12}$$

Therefore, the local bifurcation is subcritical in D/D_c and has the qualitative form as shown in Fig. 2.

The bifurcation value D_c depends on the dumbbell shape-parameter b , and on α and β defined in (2.18b) and (2.26), respectively. The values α and β were computed numerically in (2.27) for a few exponents p . In the limiting case $b - 1 = \delta \rightarrow 0^+$, we calculate from (4.5), (4.6), and (4.10), that

$$y_m \rightarrow \delta, \quad \kappa_m \rightarrow -\delta^{-3}, \quad \mathcal{G} \rightarrow 3\delta^{-1}/8, \quad \text{as} \quad \delta \rightarrow 0^+. \tag{4.13}$$

Substituting (4.13) into (4.11b), we obtain

$$D_c \sim \frac{3\beta\sqrt{\pi}}{32\alpha^2} \left(\frac{q}{p-1} \right) \left(\frac{\varepsilon}{\delta} \right)^{3/2} e^{2\delta/\varepsilon}, \quad \text{as} \quad \delta \rightarrow 0^+. \tag{4.14}$$

This limiting formula for the bifurcation point is valid for $0 < \varepsilon \ll \delta \ll 1$.

Next, we determine the global bifurcation branch for $y_0 > 0$ with $O(\varepsilon) \ll y_0 \ll y_m - O(\varepsilon)$. We set $z_0 = iv_0$ in (4.2b) with $0 < v_0 < 1$. From (4.2b) and (4.3), we then obtain

$$|\Omega| \partial_y R_{m0} = v_0 \chi_I(b; v_0), \quad (4.15)$$

where $\chi_I(b; v_0)$ is defined by

$$\begin{aligned} \chi_I(b; v_0) \equiv & \frac{(b^4 + 1)(b^2 - 1)(b^2 + v_0^2)^2}{2(b^4 - 1)^2(b^2 - v_0^2)} \\ & \times \left[\frac{(1 + b^2)}{(1 - v_0^2)(1 + b^2 v_0^2)} + \frac{2b^2}{v_0^4 - b^4} - \frac{(b^4 - 1)^2(b^2 - 1)(1 - v_0^2)(b^2 - v_0^2)}{(b^4 + 1)(1 + b^2 v_0^2)(b^2 + v_0^2)^3} \right]. \end{aligned} \quad (4.16)$$

Here $v_0 = v_0(y_0)$ is given by (4.9a). Comparing (4.15) with the local behavior (4.10), and using $y_0 \sim f'(0)v_0$ for $v_0 \ll 1$, it follows that

$$\chi_I(b; 0) = \mathcal{G}(b) f'(0), \quad (4.17)$$

where $\mathcal{G}(b)$ is defined in (4.10). As $v_0 \rightarrow 1^-$, or equivalently $y_0 \rightarrow y_m^-$, $\partial_y R_{m0} \rightarrow +\infty$. From (4.16), we calculate

$$\chi_I(b; v_0) \sim \frac{(b^4 + 1)}{4(b^2 - 1)^2} (1 - v_0)^{-1}, \quad \text{as } v_0 \rightarrow 1^-. \quad (4.18)$$

On the range $y_0 > 0$ with $O(\varepsilon) \ll y_0 \ll y_m - O(\varepsilon)$, the term in (4.7a) proportional to $e^{-2y_0/\varepsilon}$ can be neglected. To determine the dynamics of y_0 on this range, we substitute (4.7a), and (4.16), into (2.25). After some algebra, we get

$$\frac{dy_0}{dt} \sim \varepsilon^{1/2} \mu_0 e^{-2y_m/\varepsilon} \left[\left(\frac{C(y_m)}{C(r_m)} \right) \frac{e^{2y_0/\varepsilon}}{(4v_0/\varepsilon)} - \frac{D_c}{D} \left(\frac{\chi_I(b; v_0)}{\mathcal{G}(b)} \right) \right] v_0, \quad (4.19a)$$

where $r_m = y_m - y_0$. Here D_c and μ_0 are defined in (4.11), and the function $C(s)$ is defined by

$$C(s) = [s(1 - \kappa_m s)]^{1/2}. \quad (4.19b)$$

The equilibria of (4.19a) satisfy

$$\frac{D}{D_c} = 4v_0 \varepsilon^{-1} \left(\frac{C(r_m)}{C(y_m)} \right) \left(\frac{\chi_I(b; v_0)}{\mathcal{G}(b)} \right) e^{-2y_0/\varepsilon}. \quad (4.20)$$

Using the formula (4.9a) for $v_0 = v_0(y_0)$, we can write D/D_c as a function of y_0 . For $\varepsilon \ll 1$, the right-hand side of (4.20) is a decreasing function of y_0 . Thus, D is a decreasing function of y_0 .

4.2. The Lobe Region of the Dumbbell. Next, we analyze the behavior of an equilibrium spike in the right lobe \mathcal{L} of the dumbbell as D is decreased from infinity. Let \mathcal{R} denote the largest inscribed circle within \mathcal{L} . Let x_{in} and r_{in} denote the center and radius of \mathcal{R} , respectively. For $b = 1.8$, in Fig. 5 we show the right lobe \mathcal{L} and the largest inscribed circle \mathcal{R} , with center on the x -axis.

When $D = \infty$, the location x_0 of an equilibrium spike satisfies $J = 0$, where J is defined in (2.25). To leading order as $\varepsilon \rightarrow 0$, $x_0 \sim x_{\text{in}}$ satisfies $J = 0$. The correction term is of $O(\varepsilon)$ and may also be computed as in [22]. Therefore, to leading order, it suffices to determine x_{in} .

The largest inscribed circle \mathcal{R} makes two-point contact with $\partial\Omega$ at $x_c = (\xi_c, \pm\eta_c)$, with $\eta_c > 0$. These points are such that the normal to $\partial\Omega$ at x_c is parallel to the

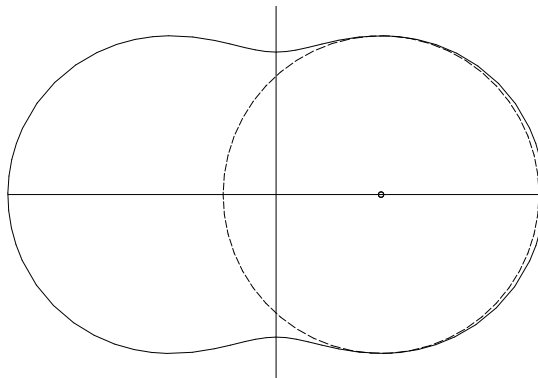


FIGURE 5. The domain Ω with $b = 1.8$ and the largest inscribed circle \mathcal{R} inside its right lobe \mathcal{L} .

y -axis. From (4.4), this implies that $\eta' = 0$. We write (4.4) as

$$\xi(t) = \frac{(b^2 - 1)^2}{\chi} \cos t, \quad \eta(t) = \frac{(b^4 - 1)}{\chi} \sin t, \tag{4.21a}$$

where

$$\chi \equiv b^4 + 1 - 2b^2 \cos(2t) = (b^2 + 1)^2 - 4b^2 \cos^2 t. \tag{4.21b}$$

Setting $\eta' = 0$, we get

$$\sin^2 t = \frac{\chi}{8b^2}, \quad \text{or} \quad \cos t = 0. \tag{4.22}$$

Two roots are $t = \pm\pi/2$. Combining (4.22) and (4.21b), we get $\chi = 2(b^2 - 1)^2$, and that the other root satisfies

$$\cos^2 t = \frac{[6b^2 - (b^4 + 1)]}{4b^2}. \tag{4.23}$$

Substituting (4.23) into (4.21), we obtain that the contact points satisfy

$$(\xi_c, \pm\eta_c) = \left(\frac{1}{4b} [6b^2 - (b^4 + 1)]^{1/2}, \pm \frac{(b^2 + 1)}{4b} \right). \tag{4.24}$$

Hence, $x_{\text{in}} = (\xi_c, 0)$, and $r_{\text{in}} = \eta_c$.

The formula (4.24) is valid only when $6b^2 - (b^4 + 1) > 0$. Therefore, we require that $1 < b < b_c \equiv 1 + \sqrt{2}$. In order to show, that r_{in} is the radius of the largest inscribed circle for this range of b , we must verify that a circle centered at x_{in} will lie strictly inside the domain, and will only touch the boundary at $(\xi_c, \pm\eta_c)$. This global verification has been done numerically.

As $b \rightarrow b_c^-$, we have $x_{\text{in}} \rightarrow (0, 0)$ and $r_{\text{in}} \rightarrow 1/\sqrt{2}$. Alternatively as $b \rightarrow 1^+$, we have $x_{\text{in}} \rightarrow (\frac{1}{2}, 0)$ and $r_{\text{in}} \rightarrow 1/4$. From (4.6) we conclude that the curvature κ_m of $\partial\Omega$ at the point $x = 0$ tends to zero as $b \rightarrow b_c^-$. Moreover, more algebra shows that the domain is convex when $b > b_c$. The convexity of the domain for $b > b_c$ explains the nonexistence of a largest inscribed circle in the right lobe of the dumbbell for this range of b .

Next, we determine the equilibrium point x_0 of (2.25a) in the right lobe of the dumbbell when D is exponentially large. In Fig. 6, we use (4.2) to plot $\partial_x R_{m0}$ along the positive x -axis. Note that $\partial_x R_{m0} > 0$ for $x > 0$. This inequality was proved in

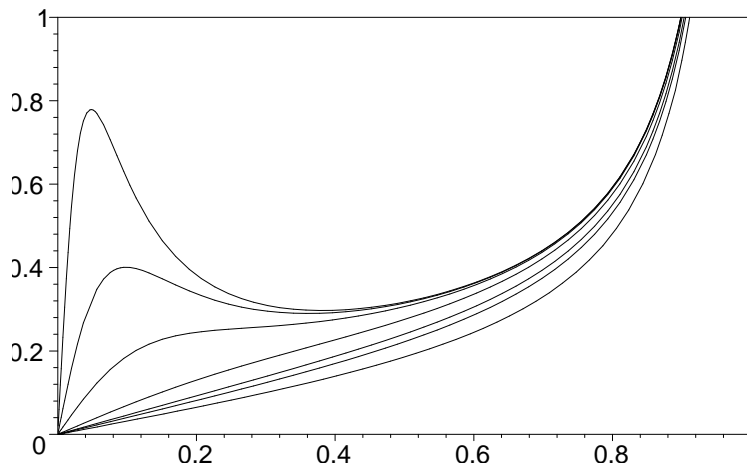


FIGURE 6. Plot of $\partial_x R_{m0}(x, 0)$ versus x for $b = 1.05, 1.1, 1.2, 1.5, 2, 2.5, \infty$. The top (bottom) curve corresponds to $b = 1.05$ (∞), respectively. Note that $\partial_x R_{m0}(x, 0)$ is positive on the positive x -axis.

[15]. Therefore, as D decreases, the equilibrium location $(x_0, 0)$ tends to the point $(1, 0) \in \partial\Omega$. When D is sufficiently small, the point $(1, 0)$ will be the closest point on the boundary to $(x_0, 0)$. In this range of D , we conclude from (2.25) that the location of the spike is determined by a balance between $\partial_x R_{m0}$ and the dominant contribution to the x -component J_1 of the integral J obtained from the closet point $(1, 0) \in \partial\Omega$. From (2.25), this unstable equilibrium satisfies

$$\frac{\alpha^2}{2\pi\beta} \left(\frac{q}{p-1} \right) J_1 = \frac{\varepsilon}{D} |\Omega| \partial_x R_{m0}. \tag{4.25}$$

Calculating J_1 asymptotically as in (3.3), we get

$$J_1 \sim 2 \left(\frac{\pi\varepsilon}{1-x_0} \right)^{1/2} \frac{e^{-2(1-x_0)/\varepsilon}}{[1-\kappa_1(1-x_0)]^{1/2}}, \tag{4.26}$$

where κ_1 is the curvature at the point $(1, 0)$ given by

$$\kappa_1 = 1 + 4b^2/(b^2 + 1)^2. \tag{4.27}$$

5. Spike Equilibria Near the Boundary. In this section we will compute the leading-order behavior of ∇R_{m0} near the boundary of the dumbbell-shaped domains of §4. We then use this formula to analyze equilibrium spike locations near the boundary. We begin with the following result, which describes the behavior of the Green's function near the boundary.

Proposition 5.1: *Let $\Omega = f(B)$, where B is the unit ball and f is given by (4.1). Let z be a point on the boundary ∂B and let $x = f(z)$ be the corresponding point on the image boundary $\partial\Omega$. Let \hat{N} be the outward pointing normal at x . Let*

$$x_0 = x - \sigma\hat{N}, \quad 0 < \sigma \ll 1, \tag{5.1}$$

and z_0 satisfy $x_0 = f(z_0)$. Then

$$\nabla R_{m0}(x_0) = \frac{\hat{N}}{4\pi\sigma} + \frac{\hat{N}}{2\pi|f'(z)|} \left[\frac{\bar{z}^2 b^2}{\bar{z}^2 b^2 - 1} - \frac{(\bar{z}^4 + 5b^2 \bar{z}^2)}{\bar{z}^4 - b^4} - \frac{1}{4} \right] + O(\sigma). \tag{5.2}$$

Here and below, ab denotes complex multiplication and $\langle a, b \rangle = \text{Re}(a\bar{b})$ will denote a vector dot product.

Proof.

We calculate \hat{N} as

$$\hat{N} = \frac{-i \frac{d}{dt} f(e^{it})}{\left| \frac{d}{dt} f(e^{it}) \right|} = \frac{zf'(z)}{|f'(z)|} = \frac{z|f'(z)|}{f'(z)}. \tag{5.3}$$

From (5.1) and (5.3) we have:

$$f(z_0) = x_0 = f(z) - \frac{\sigma z f'(z)}{|f'(z)|} \sim f\left(z - \frac{\sigma z}{|f'(z)|}\right). \tag{5.4}$$

Thus, for $0 < \sigma \ll 1$, we obtain

$$z_0 \sim z - \frac{\sigma z}{|f'(z)|} = z \left(1 - \frac{\sigma}{|f'(z)|}\right). \tag{5.5}$$

For $\sigma \ll 1$, we calculate from (4.2b) that

$$\nabla s(z_0) \sim \frac{1}{2\pi} \left(\frac{z_0}{1 - |z_0|^2}\right) + \frac{\bar{z}_0 b^2}{2\pi} \left(\frac{1}{\bar{z}_0^2 b^2 - 1} - \frac{2}{\bar{z}_0^4 - b^4}\right) + O(\sigma). \tag{5.6}$$

Substituting (5.5) into (5.6), and using $|z| = 1$, we obtain

$$\frac{1}{2\pi} \left(\frac{z_0}{1 - |z_0|^2}\right) = \frac{|f'(z)|z}{4\pi\sigma} \left(1 - \frac{\sigma}{2|f'(z)|}\right) + O(\sigma). \tag{5.7}$$

Next, we note that

$$\frac{1}{f'(z_0)} = \frac{1}{f'(z)} \left[1 + \frac{\sigma z}{|f'(z)|f'(z)} f''(z) + O(\sigma^2)\right]. \tag{5.8}$$

Therefore, using (4.1) for $f(z)$, we get

$$\frac{1}{f'(z_0)} \frac{1}{2\pi} \left(\frac{z_0}{1 - |z_0|^2}\right) = \frac{|f'(z)|z}{4\pi\sigma f'(z)} \left(1 - \frac{\sigma}{2|f'(z)|}\right) \left(1 + \frac{\sigma \bar{z} \overline{f''(z)}}{|f'(z)|f'(z)}\right) + O(\sigma), \tag{5.9a}$$

$$= \hat{N} \left(\frac{1}{4\pi\sigma} - \frac{1}{8\pi|f'(z)|} + \frac{1}{4\pi} \frac{\bar{z} \overline{f''(z)}}{|f'(z)|f'(z)}\right) + O(\sigma), \tag{5.9b}$$

$$= \hat{N} \left(\frac{1}{4\pi\sigma} - \frac{1}{8\pi|f'(z)|} + \frac{1}{4\pi|f'(z)|} \left[\frac{-2(\bar{z}^2 + 3b^2)\bar{z}^2}{\bar{z}^4 - b^4}\right]\right) + O(\sigma). \tag{5.9c}$$

Finally, substituting (5.9c) and the second term of (5.6) into (4.2a), we obtain

$$\nabla R = \frac{\nabla s(z_0)}{f'(z_0)} \quad (5.10a)$$

$$= \frac{\hat{N}}{2\pi} \left(\frac{1}{2\sigma} - \frac{1/4}{|f'(z)|} - \frac{1}{|f'(z)|} \left[\frac{(\bar{z}^2 + 3b^2)\bar{z}^2}{\bar{z}^4 - b^4} \right] \right. \\ \left. + \frac{1}{|f'(z)|} \left[\frac{\bar{z}^2 b^2}{\bar{z}^2 b^2 - 1} - \frac{2\bar{z}^2 b^2}{\bar{z}^4 - b^4} \right] \right) + O(\sigma), \quad (5.10b)$$

$$= \frac{\hat{N}}{2\pi} \left(\frac{1}{2\sigma} - \frac{1}{4|f'(z)|} + \frac{1}{|f'(z)|} \left[\frac{\bar{z}^2 b^2}{\bar{z}^2 b^2 - 1} - \frac{(\bar{z}^4 + 5b^2 \bar{z}^2)}{\bar{z}^4 - b^4} \right] \right) + O(\sigma). \quad (5.10c)$$

This completes the proof. \square

We now use this proposition to describe the spike dynamics and equilibria near the boundary. Let $x_0 = x_0(t)$ be $O(\sigma)$ close to the boundary, as defined in (5.1), and assume that $\varepsilon \ll \sigma \ll 1$. We then use Laplace's method to calculate the integral J in (2.25a) as

$$J \sim 2\sqrt{\frac{\pi\varepsilon}{\sigma}} e^{-2\sigma/\varepsilon} \hat{N}, \quad (5.11)$$

where J is defined in (2.25b). In deriving (5.11) we have assumed that $\kappa\sigma \ll 1$, where κ is the curvature of $\partial\Omega$. Substituting (5.11) and (5.10c) into (2.25a), we obtain

$$\frac{dx_0}{dt} \sim \frac{2\varepsilon q}{p-1} \left[\frac{\alpha^2}{\pi\beta} \left(\frac{p-1}{q} \right) \sqrt{\frac{\pi\varepsilon}{\sigma}} e^{-2\sigma/\varepsilon} \hat{N} \right. \\ \left. - \frac{\varepsilon|\Omega|}{D} \left\{ \frac{\hat{N}}{4\pi\sigma} - \frac{\hat{N}}{8\pi|f'(z)|} + \frac{\hat{N}}{2\pi|f'(z)|} \left(\frac{\bar{z}^2 b^2}{\bar{z}^2 b^2 - 1} - \frac{\bar{z}^4 + 5b^2 \bar{z}^2}{\bar{z}^4 - b^4} \right) \right\} \right]. \quad (5.12)$$

Note that the first three terms on the right hand side of (5.12) point in the direction of \hat{N} . Therefore, a necessary condition for x_0 to be in equilibrium is that the last term on the right hand-side of (5.12) also points in the normal direction, i.e.

$$\text{Im} \left(\frac{\bar{z}^2 b^2}{\bar{z}^2 b^2 - 1} - \frac{\bar{z}^4 + 5b^2 \bar{z}^2}{\bar{z}^4 - b^4} \right) = 0. \quad (5.13)$$

This condition is clearly satisfied when $z = \pm 1$ and when $z = \pm i$. Next we show that there are no other solutions to (5.13). Setting $w = z^2$ and using $2\text{Im}(x) = x - \bar{x}$, (5.13) becomes

$$-\frac{(\bar{w}^2 + 5b^2 \bar{w})}{\bar{w}^2 - b^4} + \frac{\bar{w} b^2}{\bar{w} b^2 - 1} + \frac{w^2 + 5b^2 w}{w^2 - b^4} - \frac{w b^2}{w b^2 - 1} = 0. \quad (5.14)$$

Using the relation $w\bar{w} = 1$, (5.14) simplifies to

$$4(1 + b^4)b^2 \frac{w(w-1)(w+1)}{(b^4 w^2 - 1)(b^4 - w^2)} = 0. \quad (5.15)$$

It follows $z = \pm 1, \pm i$. are the only possible equilibria.

When the condition (5.13) is satisfied, we obtain to leading order from (5.12) that the equilibrium location for σ is related to D by

$$D \sim \frac{\beta}{4\alpha^2} \left(\frac{q}{p-1} \right) \left(\frac{\varepsilon}{\pi\sigma} \right)^{1/2} |\Omega| e^{2\sigma/\varepsilon}. \tag{5.16}$$

Notice that this relation is the same for any equilibrium location. Moreover, (5.16) involves only the leading order behavior of $\nabla R \sim \frac{\hat{N}}{4\pi\sigma}$ near the boundary, which is independent of the shape of the boundary. Therefore, the result (5.16) is also independent of the domain shape. Notice also that (5.16) with $|\Omega| = \pi$ agrees with the result (3.15) derived earlier for an equilibrium spike near the boundary of a circular cylindrical domain of radius one.

Next, we analyze the stability of these equilibria with respect to the direction normal to the boundary. Notice that $D = D(\sigma)$ has a minimum at $\sigma_m = \frac{\varepsilon}{4}$. At this point, $D(\sigma_m) \equiv D_m = \sqrt{2}e^{\frac{1}{2}} \frac{|\Omega|q\beta}{4\alpha^2\sqrt{\pi}(p-1)}$. However, since we have assumed that $\sigma \gg \varepsilon$, we have $D \gg D_m$. Furthermore, for any given D with $D \gg D_m$, (5.16) has two solutions for σ : $\sigma_1 \ll \varepsilon$ and $\sigma_2 \gg \varepsilon$. By examining the sign of the right hand side of (5.12), we conclude that the equilibrium at σ_2 is *unstable* with respect to the normal direction. Alternatively, σ_1 is stable with respect to the normal direction. However, our analysis is invalid for the root σ_1 , since $\sigma_1 \ll \varepsilon$. Nevertheless, this formal analysis may suggest the existence of boundary spike equilibria located on the boundary of $\partial\Omega$ at $f(z)$, where $z = \pm 1$ or $z = \pm i$. See Conjecture 7.1 below.

Next, we analyze the stability of these equilibria with respect to the tangential direction. The unit tangent vector to $\partial\Omega$, measured in the counterclockwise direction, is

$$\hat{T}(t) = i \frac{z f'(z)}{|f'(z)|} \quad \text{where } z = e^{it}. \tag{5.17}$$

The stability in the tangential direction is controlled by the last term on the right hand side of (5.12). The direction of this term, up to a positive constant scalar multiple, is given by

$$\vec{v}(t) = -\frac{1}{|f'(z)|} \hat{N} \left(\frac{\bar{z}^2 b^2}{\bar{z}^2 b^2 - 1} - \frac{(\bar{z}^4 + 5b^2 \bar{z}^2)}{\bar{z}^4 - b^4} \right), \tag{5.18a}$$

$$= -\frac{f'(z)}{|f'(z)|^2} \left(\frac{\bar{z} b^2}{\bar{z}^2 b^2 - 1} - \frac{(\bar{z}^3 + 5b^2 \bar{z})}{\bar{z}^4 - b^4} \right), \tag{5.18b}$$

where $z = e^{it}$.

The differential equation (5.12) can be written in the form

$$\frac{dx_0}{dt} \sim a_1 \hat{N} + \omega \vec{v}, \tag{5.19}$$

where a_1 and $\omega > 0$ are real. Multiplying (5.19) by \hat{T} and taking real parts of the resulting expression we get

$$\text{Re} \left(x_0' \hat{T} \right) = \omega \text{Re} \left(\vec{v} \hat{T} \right). \tag{5.20}$$

We decompose the velocity field as $x_0' = s_N \hat{N} + s_T \hat{T}$, and we let θ denote the angle between the tangential direction and \vec{v} . Using the identity $\langle a, b \rangle = \text{Re}(a\bar{b})$ for the dot product, we then reduce (5.20) to

$$s_T = \omega |\vec{v}| \cos \theta, \tag{5.21}$$

where

$$\cos \theta = \frac{1}{|\vec{v}|} \langle \hat{T}, \vec{v} \rangle, \quad (5.22a)$$

$$= \frac{1}{|\vec{v}|} \operatorname{Re} \left[i \frac{z f'(z) \overline{f'(z)}}{|f'(z)| |f'(z)|^2} \left(\frac{z^3 + 5b^2 z}{z^4 - b^4} - \frac{z b^2}{z^2 b^2 - 1} \right) \right], \quad (5.22b)$$

$$= -C(t) \operatorname{Im} \left(\frac{z^4 + 5b^2 z^2}{z^4 - b^4} - \frac{z^2 b^2}{z^2 b^2 - 1} \right). \quad (5.22c)$$

Here $C(t)$ is some irrelevant positive scalar.

At the equilibrium points $z = \pm 1$ and $z = \pm i$ we have that \vec{v} points in the normal direction. Therefore, at these points, we have $\langle \hat{T}, \vec{v} \rangle = 0$ and $\cos \theta = 0$. From (5.21) we observe that if $\frac{d \cos \theta}{dt} < 0$ at the equilibrium position, then we have stability in the tangential direction. At the equilibrium positions, where $\sin \theta = 1$, we calculate from (5.22) that

$$\frac{d\theta}{dt} = C(t) \operatorname{Im} \left[\frac{d}{dt} \mathcal{F}(e^{it}) \right], \quad \text{where } \mathcal{F}(z) \equiv \frac{z^4 + 5b^2 z^2}{z^4 - b^4} - \frac{z^2 b^2}{z^2 b^2 - 1}. \quad (5.23)$$

At $t = 0$ and $t = \pi/2$ where $z = 1$ and $z = i$, respectively, we obtain from (5.23) that

$$\left. \frac{d\theta}{dt} \right|_{t=0} = C(0) \operatorname{Re} [\mathcal{F}'(0)], \quad \left. \frac{d\theta}{dt} \right|_{t=\frac{\pi}{2}} = -C \left(\frac{\pi}{2} \right) \operatorname{Im} [\mathcal{F}'(i)]. \quad (5.24)$$

From (5.23) and (5.24), we calculate

$$\left. \frac{d\theta}{dt} \right|_{t=0} = -C(0) \left(\frac{8b^2(1+b^4)}{(b^2+1)^2(b^2-1)^2} \right) < 0, \quad (5.25a)$$

$$\left. \frac{d\theta}{dt} \right|_{t=\frac{\pi}{2}} = C \left(\frac{\pi}{2} \right) \left(\frac{8b^2(1+b^4)}{(b^2+1)^2(b^2-1)^2} \right) > 0. \quad (5.25b)$$

Since $\frac{d \cos \theta}{dt} = -\frac{d\theta}{dt}$ at the equilibrium positions, we conclude from (5.21) and (5.25) that the equilibrium position near $f(\pm i)$ (near $f(\pm 1)$) is stable (unstable) in the tangential direction, respectively. We summarize our results in the following proposition.

Proposition 5.2: *For the dumbbell-shaped domain $\Omega = f(B)$, where f is given by (4.1), let σ be such that $\varepsilon \ll \sigma \ll 1$. For the value of D given by (5.16), there are precisely four equilibrium spike locations, all at a distance σ away from the boundary. They are given by $x_s^\pm = f(\pm i) - \hat{N}\sigma$ and $x_u^\pm = f(\pm 1) - \hat{N}\sigma$, where \hat{N} is the normal to the boundary $\partial\Omega$ at $f(\pm i)$ and $f(\pm 1)$, respectively. All four equilibria are unstable in the direction \hat{N} normal to the boundary. Moreover, x_s^\pm (x_u^\pm) are stable (unstable) in the tangential direction, respectively.*

In Fig. 7 we illustrate the local vector field and stability properties of near-boundary spikes. Our results suggest that the unstable manifold of the equilibrium near-boundary spike along the x -axis connects with the stable manifold of the near-boundary spike along the y -axis in the neck region of the dumbbell.

Our analysis has been restricted to the case where the distance σ between the spike and the boundary satisfies $\sigma \gg \varepsilon$. We expect that the equilibrium locations of spikes that are located on the boundary of the domain should result from a competition between the zeroes of the derivative of the curvature (as for the shadow

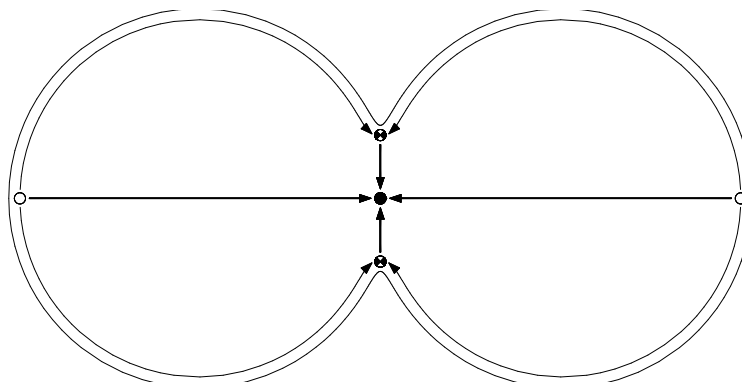


FIGURE 7. Plot of local vector field associated with near-boundary spikes for the dumbbell-shaped domain of §4.

problem where $D = \infty$) and the local behavior of the gradient of the regular part R_m of the Green's function on the boundary. To this end, we define R_b by

$$R_b(x) = \lim_{y \rightarrow x} \left[R_m(x, y) + \frac{1}{4\pi} \ln |x - y| \right]. \tag{5.26}$$

We now show that for the dumbbell-shaped domain of §4 that the minimum of R_b occurs at that point of the boundary where the curvature is at its minimum.

For the dumbbell-shaped domains of §4 we obtain the following result:

Proposition 5.3: *Let $\Omega = f(B)$ where f is given by (4.1) and B is the unit ball. Then R_b defined in (5.26) is given by:*

$$R_b(x) = \frac{1}{4\pi} \ln \left(\frac{b^4 + 2b^2 \cos 2t + 1}{b^4 - 2b^2 \cos 2t + 1} \right) + C, \quad \text{where } x = f(e^{it}). \tag{5.27}$$

Here C is some constant independent of x .

The proof of this result is given in Appendix A. Notice that the expression inside the log term of (5.27) has its maximum at $t = 0, \pi$ and its minimum at $t = \frac{\pi}{2}, \frac{3\pi}{2}$. Therefore, R_b has a minimum on the y axis in the neck of the dumbbell, where the curvature of $\partial\Omega$ is at its minimum.

6. Bifurcations in a Dumbbell-Shaped Domain when $D = O(1)$. In this section, for $D = O(1)$, we compute numerically the location of a one-spike equilibrium solution to (1.1) for the one-parameter family of dumbbell-shaped domains generated by the mapping (4.1) of the unit disk. The following result, derived in [15], characterizes the motion of a one-spike solution to (1.1) when $\tau = 0$ in (1.1b):

Proposition 6.1 (From [15]): *Let $\varepsilon \ll 1$, $x_0 \in \Omega$, with $\text{dist}(x_0; \partial\Omega) \gg O(\varepsilon)$, and suppose that $\varepsilon^2 \ll D \ll -\log \varepsilon$. Then, the location $x = x_0(t)$ of a one-spike solution to (1.1) with $\tau = 0$ satisfies the differential equation*

$$\frac{dx_0}{dt} \sim - \left(\frac{4\pi q}{p-1} \right) \frac{\varepsilon^2}{-\log \varepsilon + 2\pi R_0} \nabla R_0, \tag{6.1a}$$

where R_0 and its gradient are defined by

$$R_0 \equiv R(x_0, x_0), \quad \nabla R_0 \equiv \nabla_x R(x, x_0)|_{x=x_0}. \tag{6.1b}$$

Here R is the regular part of the reduced wave Green's function defined by (1.6).

From (6.1), the spike equilibria satisfy

$$\nabla R_0 = 0. \quad (6.2)$$

For the one-parameter family of dumbbell-shaped domains of §4, there should be three roots to (6.2) when D is sufficiently small since, in this limit, R_0 is determined by the distance function. When $D \ll 1$, local minima of R_0 , which correspond to local maxima of the distance function (cf. [15]), are stable equilibria under (6.1). Hence, when $D \ll 1$ and for the one-parameter family of dumbbell-shaped domains of §4, there should be a stable spike equilibrium in each lobe of the dumbbell. There is an unstable spike equilibrium at the origin, which corresponds to a saddle point of R_0 (see Fig. 1(f) above). However, as discussed in §4, when $D \gg 1$ but with D not exponentially large as $\varepsilon \rightarrow 0$, there should only be a stable spike equilibrium at the origin.

The goal here is to numerically study a bifurcation that occurs for $D = O(1)$ where the spike at the origin loses its stability to stable spike solutions that migrate towards the lobes of the dumbbell as D is decreased below the bifurcation point. Such a bifurcation was first observed numerically in [15] for a particular dumbbell-shaped domain not of the type (4.1). Here, we consider the dumbbell-shaped domains generated by (4.1) as a function of both the shape-parameter $b > 1$ of (4.1) and of $\lambda = D^{-1/2}$. The bifurcation diagrams that we compute for these domains are significantly more complicated than in [15], in that we find that for some ranges of b the bifurcation can be either subcritical or supercritical in the parameter $\lambda \equiv D^{-1/2}$ (see Fig. 1(d) and Fig. 1(e) above).

Since we cannot calculate R_0 using complex variable methods, we determine the roots of (6.2) numerically using a boundary element method to compute the regular part R of (1.6). Before describing our numerical results, we outline this boundary element method.

6.1. Boundary Element method. We now describe the Boundary Element method (BEM) used to compute the regular part $R(x, x_0)$ for (1.6). In (1.6), we set

$$G(x, x_0) = V(x, x_0) + \tilde{R}(x, x_0), \quad V(x, x_0) \equiv \frac{1}{2\pi} K_0(\lambda|x - x_0|). \quad (6.3)$$

Here $K_0(z)$ is the modified Bessel function of order zero. By comparing (1.6c) with (6.3), we get

$$\tilde{R}(x, x_0) = R(x, x_0) + \frac{1}{2\pi} [\log|x - x_0| + K_0(\lambda|x - x_0|)]. \quad (6.4a)$$

Then, using the local behavior of $K_0(z)$, we obtain

$$\tilde{R}(x, x_0) = R(x, x_0) - \frac{1}{2\pi} (\log 2 - e - \log \lambda) + o(1), \quad \text{as } x \rightarrow x_0, \quad (6.4b)$$

where e is Euler's constant. Therefore, since $\nabla \tilde{R}(x; x_0)|_{x=x_0} = \nabla R(x; x_0)|_{x=x_0}$, it suffices to compute $\tilde{R}(x, x_0)$.

Substituting (6.3) into (1.6a) and (1.6b), we obtain that $\tilde{R}(x, \xi)$ satisfies

$$\Delta \tilde{R}(x, \xi) - \lambda^2 \tilde{R}(x, \xi) = 0, \quad x \in \Omega, \quad (6.5a)$$

$$\partial_n \tilde{R}(x, \xi) = -\partial_n V(x, \xi), \quad x \in \partial\Omega. \quad (6.5b)$$

The integral representation for \tilde{R} is

$$\tilde{R}(x, \xi) = - \int_{\partial\Omega} G(x, \eta) \partial_n V(\eta, \xi) dS(\eta). \tag{6.6a}$$

Using (6.3), this can be written as

$$\tilde{R}(x, \xi) = - \int_{\partial\Omega} \tilde{R}(x, \eta) \partial_n V(\eta, \xi) dS(\eta) - \int_{\partial\Omega} V(x, \eta) \partial_n V(\eta, \xi) dS(\eta). \tag{6.6b}$$

Next, we discretize the boundary $\partial\Omega$ into n pieces $\partial\Omega_1, \dots, \partial\Omega_n$, and approximate $\tilde{R}(x, \xi) = \tilde{R}(x, \xi_i)$ for $\xi_i \in \partial\Omega_i$, where ξ_i is the midpoint of the arc $\partial\Omega_i$. Letting $\tilde{R}_j = \tilde{R}(x, \xi_j)$, we can then approximate (6.6b) by the dense linear system

$$\tilde{R}_j = \sum_{i=1}^n \left(a_{ij} \tilde{R}_i + b_{ij} \right), \tag{6.7a}$$

where

$$a_{ij} = - \int_{\partial\Omega_i} \partial_n V(\eta, \xi_j) dS(\eta), \quad b_{ij} = - \int_{\partial\Omega_i} V(x, \eta) \partial_n V(\eta, \xi_j) dS(\eta). \tag{6.7b}$$

After calculating the solution to (6.7a), we can determine $\tilde{R}(x, x_0)$ by discretizing (6.6b). This leads to

$$\tilde{R}(x, x_0) = - \sum_{i=1}^n \left(V(x, \eta_i) + \tilde{R}_i \right) \partial_n V(\eta_i, x_0) l_i. \tag{6.8}$$

Here l_i is the length of $\partial\Omega_i$.

It remains to compute the coefficients a_{ij} and b_{ij} in (6.7b). When $i \neq j$ we have

$$a_{ij} = -l_i \partial_n V(\eta_i, \xi_j), \quad b_{ij} = -l_i V(x, \eta_i) \partial_n V(\eta_i, \xi_j). \tag{6.9}$$

The case $i = j$ requires a special treatment because of the logarithmic singularity of the free-space Green's function V . Let r be the radius of curvature of $\partial\Omega_i$ at ξ_i , and set $\kappa_i = 1/r$. Let $l = l_i$ be the length of $\partial\Omega_i$. Since $\partial\Omega_i$ is small, we may assume that $\partial\Omega_i$ is parametrized for $t \ll 1$ as

$$\eta(t) = r(\cos t, \sin t), \quad -\frac{l}{2r} \leq t \leq \frac{l}{2r}, \tag{6.10a}$$

with

$$\xi = \xi_i = (r, 0). \tag{6.10b}$$

The asymptotic behavior $V(\eta, \xi) \sim -\frac{1}{2\pi} \log |\eta - \xi| + O(1)$ as $|\eta - \xi| \rightarrow 0$ yields

$$\partial_n V(\eta, \xi) \sim -\frac{1}{2\pi} \frac{\eta - \xi}{|\eta - \xi|^2} \cdot \hat{n}. \tag{6.11}$$

Since $\hat{n} = (\cos t, \sin t)$ we calculate $(\eta - \xi) \cdot \hat{n} = r(1 - \cos t)$, and $|\eta - \xi|^2 = r^2(2 - 2 \cos t)$. Hence, from (6.11),

$$\partial_n V(\eta, \xi) \sim -\frac{1}{4\pi r}, \quad \text{as } r \rightarrow 0, \tag{6.12}$$

Therefore, the coefficients a_{ii} and b_{ii} in (6.7b) are

$$a_{ii} = \frac{\kappa_i}{4\pi} l_i, \quad b_{ii} = a_{ii} V(x, \eta_i). \tag{6.13}$$

6.2. Numerical Results For Spike Equilibria. We now discuss our numerical results. In the computations below we took roughly 200 boundary elements. Since Ω is symmetric we look for spike equilibria that are along the x -axis.

When the dumbbell shape-parameter is $b = 1.2$, and for the values of λ as shown, in Fig. 8a we plot R_x along the segment of the positive x -axis that lies within the dumbbell. Notice that there are either one, two, or three spike equilibria on $x \geq 0$ depending on the range of λ . The resulting subcritical pitchfork bifurcation diagram for the spike equilibria is shown in Fig. 8b. Our computations show that there is a pitchfork bifurcation at $\lambda \approx 3.74$. Furthermore, there is a fold-point bifurcation of spike equilibria when $\lambda \approx 2.59$. The spike at the origin is stable when $\lambda < 3.74$, and is unstable for $\lambda > 3.74$. In Fig. 8b, the upper branch of spike equilibria is stable, while the middle branch is unstable. A subcritical bifurcation diagram of this type has not computed previously. Notice that as $\lambda \rightarrow \infty$ ($D \rightarrow 0$), the upper branch corresponds to stable spike equilibria that tend to the lobes of the dumbbell as $D \rightarrow 0$.

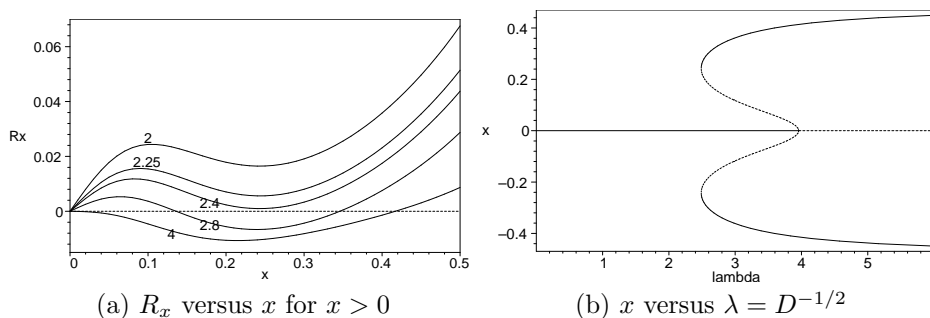


FIGURE 8. (a) Plot of R_x when x is along the positive real axis, for the values of λ as indicated. The dumbbell shape-parameter is $b = 1.2$. (b) The subcritical bifurcation diagram of the roots of $R_x = 0$ versus $\lambda = D^{-1/2}$ when $b = 1.2$.

Next, we investigate numerically the effect of changing the dumbbell shape-parameter b . In Fig. 9 we plot the numerically computed bifurcation diagram of spike equilibria for nine different values of b . The leftmost curve in this figure correspond to $b = 1.15$. Successive curves, from left to right in Fig. 9, correspond to an increment in b of 0.05. Qualitatively, we observe from this figure that the equilibrium spike at the origin has a subcritical bifurcation in λ only when $1 < b < b_c$. For $b > b_c$, the origin has a more conventional supercritical pitchfork bifurcation. We estimate numerically that $b_c \approx 1.4$. Since for $b \rightarrow 1^+$ the domain Ω reduces to the union of two disconnected circles each of radius $1/2$, Fig. 9 suggests that the bifurcation of spike equilibria at the origin is subcritical when the neck of the dumbbell is sufficiently narrow, and is supercritical when the domain is close to a unit circle (b large). It would be interesting to investigate more generally whether certain broad classes of dumbbell-shaped domains with thin necks will always yield subcritical pitchfork bifurcations for a one-spike equilibrium of (1.1) when $D = O(1)$. We remark that the stability properties of the branches of equilibria in Fig. 9 are precisely the same as described previously for Fig. 9. For each $b > 1$, there is still a stable spike equilibrium that tends to a lobe of the dumbbell as $\lambda \rightarrow \infty$ ($D \rightarrow 0$).

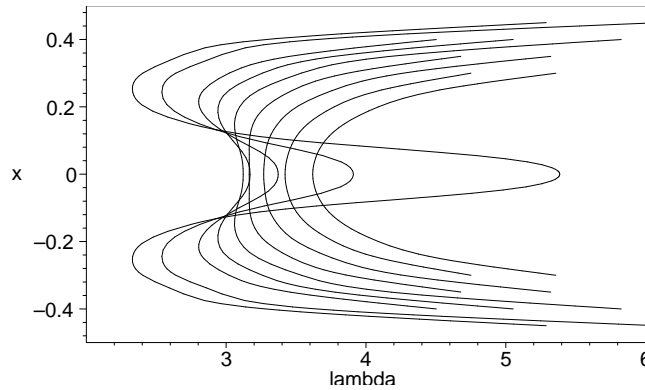


FIGURE 9. Plot of the bifurcation diagram for the spike equilibria versus $\lambda = D^{-1/2}$ for various values of the dumbbell shape-parameter b . The curves from left to right correspond to $b = 1.15$, $b = 1.2$, $b = 1.25$, $b = 1.3$, $b = 1.35$, $b = 1.4$, $b = 1.45$, $b = 1.5$, and $b = 1.55$.

In Fig. 10a we plot the bifurcation diagram in the λ versus b parameter plane. From this figure we observe that when $b > 1.4$, there is only one bifurcation value of λ , and it corresponds to the pitchfork bifurcation point for the equilibrium $x_0 = 0$. For $1.15 < b < 1.4$, there are two bifurcation values for λ . The larger value of λ corresponds to the pitchfork bifurcation value, and the smaller value of λ corresponds to the fold-point value where the middle and upper branches of spike equilibria associated with the subcritical bifurcation coincide. Finally, in Fig. 10b, we plot the fold-point value for the spike equilibria as a function of b for $1.15 < b < 1.4$. The non-smoothness of this curve reflects the fact that, due to computational resource limitations, we only had nine data points to fit with a spline interpolation.

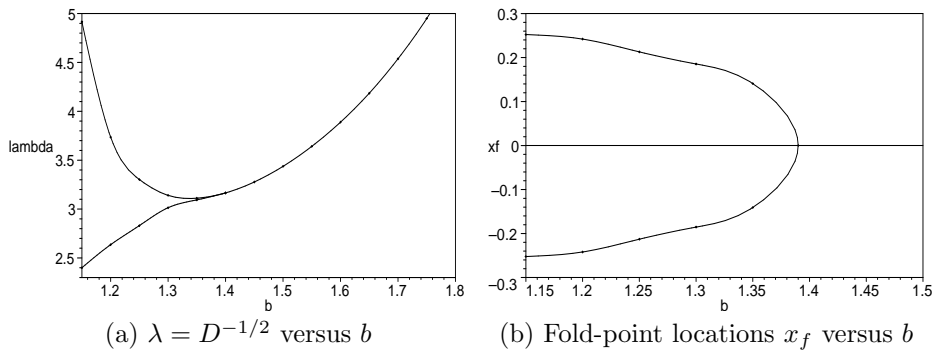


FIGURE 10. (a) Curves of λ versus b where the spike equilibria have either a pitchfork bifurcation or a fold-point bifurcation. (b) Locations x_f of the fold-point bifurcation versus b .

7. Discussion. For different ranges of the inhibitor diffusivity D , we have described the bifurcation behavior of an equilibrium one-spike solution to the GM

model (1.1) in a one-dimensional domain, in a radially symmetric domain, and in a class of dumbbell-shaped domains. On a one-dimensional interval and in a radially symmetric domain, we have calculated the bifurcation value $D_c = O(\varepsilon^2 e^{2d/\varepsilon})$, where d is the distance of the spike to the boundary, for which an equilibrium spike at the midpoint of the domain becomes stable as D decreases below D_c . For a dumbbell-shaped domain, we have shown that the qualitative bifurcation diagram of Fig. 1 for interior spike solutions holds. In §4 we found that an unstable spike in the neck of the dumbbell becomes stable through a pitchfork bifurcation when D decreases below some asymptotically exponentially large value. Since this bifurcation occurs when D is exponentially large as $\varepsilon \rightarrow 0$, a main conclusion of our study is that spike behavior for the shadow system corresponding to $D = \infty$, has very different properties from that of spike solutions to (1.1) when D is large, but independent of ε . Moreover, in §6, we showed that when D decreases below some $O(1)$ value, the spike in the neck of the dumbbell loses its stability through a pitchfork bifurcation to two stable spike locations that tend to the lobes of the dumbbell as $D \rightarrow 0$.

There are several open problems that await a rigorous proof. A main conjecture, formulated in [15] and explored further here, is that the gradient ∇R_m of the regular part of the modified Green's function with *Neumann* boundary conditions has a unique root in an arbitrary, possibly non-convex, simply-connected bounded domain. In contrast, as was shown in [10], this is not true if *Dirichlet* boundary conditions are used instead. Many properties of the gradient of the regular part of the Green's function for the Laplacian with *Dirichlet* boundary condition have been given in the survey [2]. The uniqueness of a root to this gradient with *Dirichlet* boundary conditions in a *convex* domain is established in [10] and [4]. Our conjecture shows that further work is needed to understand the properties of the regular part of the Green's function associated with a *Neumann* boundary condition.

A second conjecture, based on §6, is that the zeroes of the gradient ∇R of the reduced wave Green's function will have a subcritical bifurcation with respect to $\lambda = D^{-1/2}$ in a dumbbell-shaped domain, whenever the neck of the dumbbell is sufficiently thin. Alternatively, we conjecture that the zeroes of ∇R will have a supercritical bifurcation in λ when a dumbbell-shaped domain is sufficiently close to a circular domain.

Although there have been many studies of the existence and stability of boundary spikes for the shadow GM system with $D = \infty$, the problem of constructing equilibrium boundary spike solutions for different ranges of D is largely open. The analysis in this paper has been restricted to the situation where the spike is away from the boundary, i.e. the distance σ of a spike to the boundary is such that $\sigma \gg O(\varepsilon)$. Therefore, we have not described boundary spikes or spikes that are $O(\varepsilon)$ close to the boundary. Some work on equilibrium boundary spikes for the case where D is algebraically large as $\varepsilon \rightarrow 0$ is given in [7].

For the case where $D = \infty$, the dynamical behavior of a boundary spike was derived in [13]. The equilibrium case was studied in [25] and [27] (see also the references therein). From these studies, it is well-known that the dynamics and equilibrium locations depend only on the curvature of the boundary of the domain. For the domain in Fig. 1, the boundary spike located on the y -axis is stable when $D = \infty$. For asymptotically large values of D , we expect that the dynamics of a boundary spike depends on both the derivative of the curvature of the boundary and on the behavior of the gradient of the regular part of the Green's function R_m

on the boundary. For the dumbbell-shaped domain of §4, we showed in §5 that this gradient vanishes at the same points where the curvature of the boundary has a local maxima or minima. This suggests the following conjecture:

Conjecture 7.1: *Suppose that $O(1) \ll D \ll O(\varepsilon^q e^{c/\varepsilon})$ for some q and c to be found. Then, a boundary spike for the domain $\Omega = f(B)$ shown in Fig. 1 is at equilibrium if and only if its center is located on either the x or the y -axes. Furthermore, the equilibrium locations on the y and the x -axes are stable and unstable, respectively.*

Finally, it is well-known (cf. [3], [16], [9]) that the shadow system admits unstable multi-spike equilibrium solutions where the locations of the spikes satisfy a ball-packing problem. These solutions are unstable with respect to both the large $O(1)$ and the exponentially small eigenvalues of the linearization. Since when $D \ll 1$, the distance function plays a central role, the locations of the spikes should also satisfy a ball packing problem. However, in a strictly convex domain these solutions should be stable. It would be interesting to extend the analysis given here to determine the bifurcation properties, and the exchange of stability, of multi-spike solutions as D is decreased.

Acknowledgements. T. Kolokolnikov was supported by an NSERC graduate fellowship. M. J. W. is grateful for the support of NSERC under grant 81541. We also would like to thank one of the referees for their detailed reading of the manuscript.

Appendix A. The Proof of Proposition 5.3. Here we prove Proposition 5.3. Let $x = x(t) = f(e^{it})$, \hat{N} be the normal at x , and label $y(t) = x(t) - \sigma\hat{N}(t)$. We define $h(t)$ by

$$h(t) = R_m(y(t), y(t)), \tag{A.1}$$

and calculate

$$h'(t) = \nabla R_m(y(t), y(t)) \cdot y'(t). \tag{A.2}$$

Note that $x'(t) = \hat{T}|f'(z)|$, where $z = e^{it}$ and $\hat{T} = i\hat{N}$ is the tangential direction at $x = f(z)$. Therefore, we have

$$y'(t) = |f'(z)|\hat{T} - \sigma c\hat{T}, \tag{A.3}$$

where $c(t) = \frac{d}{dt}|\hat{N}|$ is some irrelevant function. From Proposition 5.1 and using $a \cdot b = \text{Re}(\bar{a}b)$, we obtain

$$\begin{aligned} h'(t) &= \left(\frac{\hat{N}}{4\pi\sigma} + \frac{\hat{N}}{2\pi|f'(z)|} \left[\frac{\bar{z}^2 b^2}{\bar{z}^2 b^2 - 1} - \frac{(\bar{z}^4 + 5b^2 \bar{z}^2)}{\bar{z}^4 - b^4} - \frac{1}{4} \right] + O(\sigma) \right) \\ &\quad \cdot \left(\hat{T}|f'(z)| - \sigma c\hat{T} \right) \\ &= -\frac{1}{2\pi} \text{Im} \left[\frac{z^2 b^2}{z^2 b^2 - 1} - \frac{(z^4 + 5b^2 z^2)}{z^4 - b^4} \right] + O(\sigma) = \frac{1}{2\pi} \text{Im} \mathcal{F}(z), \end{aligned} \tag{A.4}$$

where \mathcal{F} is given by (5.23). Note that the singular part $\frac{\hat{N}}{4\pi\sigma}$ does not enter into $h'(t)$ since it is perpendicular to the tangent direction.

Integrating (A.4), we obtain

$$h(t) = \int h'(t)dt = \frac{1}{2\pi} \int \text{Im} \mathcal{F}(z) \frac{dz}{iz}. \tag{A.5}$$

Therefore,

$$\operatorname{Im} \mathcal{F}(z) = \frac{\mathcal{F}(z) - \mathcal{F}(\frac{1}{z})}{2i} \quad (\text{A.6a})$$

$$= \frac{1}{i} 2(1 + b^4)b^2 \frac{w(w^2 - 1)}{(b^4w^2 - 1)(w^2 - b^4)}, \quad (\text{A.6b})$$

$$= \frac{-1}{i} w \left(\frac{b^2}{wb^2 + 1} - \frac{b^2}{wb^2 - 1} + \frac{1}{w + b^2} - \frac{1}{w - b^2} \right). \quad (\text{A.6c})$$

Here $w = z^2$. In addition, $\frac{dz}{z} = \frac{1}{2} \frac{dw}{w}$ so that

$$h(t) = \frac{1}{4\pi} \int \left(\frac{b^2}{wb^2 + 1} - \frac{b^2}{wb^2 - 1} + \frac{1}{w + b^2} - \frac{1}{w - b^2} \right) dw, \quad (\text{A.7a})$$

$$= \frac{1}{4\pi} \ln \left| \frac{(wb^2 + 1)(w + b^2)}{(wb^2 - 1)(w - b^2)} \right| + C. \quad (\text{A.7b})$$

This result can be simplified as

$$h(t) = \frac{1}{4\pi} \ln \left| \frac{(wb^2 + 1)(w + b^2)}{(wb^2 - 1)(w - b^2)} \right| + C, \quad (\text{A.8a})$$

$$= \frac{1}{8\pi} \ln \frac{(wb^2 + 1)(\bar{w}b^2 + 1)(w + b^2)(\bar{w} + b^2)}{(wb^2 - 1)(\bar{w}b^2 - 1)(w - b^2)(\bar{w} - b^2)} + C, \quad (\text{A.8b})$$

$$= \frac{1}{8\pi} \ln \frac{(1 + b^4 + 2b^2 \cos 2t)^2}{(1 + b^4 - 2b^2 \cos 2t)^2} + C, \quad (\text{A.8c})$$

$$= \frac{1}{4\pi} \ln \left(\frac{1 + b^4 + 2b^2 \cos 2t}{1 + b^4 - 2b^2 \cos 2t} \right) + C. \quad (\text{A.8d})$$

The constant $C = C(\sigma)$ depends on the distance from the boundary but not on x . Finally, for $x \in \partial\Omega$ and $y \in \Omega$, we define the regular part of the boundary Green's function by

$$S(x, y) = R_m(x, y) + \frac{1}{4\pi} \ln |x - y|. \quad (\text{A.9})$$

Note that S is smooth and bounded for all $y \in \Omega$. Therefore, we have

$$R_b(x) = \lim_{y \rightarrow x} S(x, y) = \lim_{y \rightarrow x} [S(y, y) + O(x - y)] = \lim_{y \rightarrow x} S(y, y), \quad (\text{A.10a})$$

$$= \lim_{\sigma \rightarrow 0} h(t) + \frac{1}{4\pi} \ln \sigma \quad (\text{A.10b})$$

$$= \frac{1}{4\pi} \ln \left(\frac{1 + b^4 + 2b^2 \cos 2t}{1 + b^4 - 2b^2 \cos 2t} \right) + C. \quad (\text{A.10c})$$

Since we are only concerned with determining points on the boundary where R_b has minima and maxima, the constant C is irrelevant. This completes the proof. \square

REFERENCES

- [1] M. Abramowitz, I. Stegun, *Handbook of Mathematical Functions*, Dover Publications, New York, (1965).
- [2] C. Bandle, M. Flucher, *Harmonic Radius and Concentration of Energy; Hyperbolic Radius and Liouville's Equations $\Delta U = e^U$ and $\Delta U = U^{(n+2)/(n-2)}$* , SIAM Rev., **38**, No. 2, (1996), pp. 191–238.
- [3] P. Bates, N. Fusco, *Equilibria with Many Nuclei for the Cahn-Hilliard Equation*, J. Diff. Eq., **160**, No. 2, (2000), pp. 283–356.

- [4] L. A. Caffarelli, A. Friedman, *Convexity of Solutions of Semilinear Elliptic Equations*, Duke Math. J., **52**, No. 2, (1985), pp. 431–456.
- [5] X. Chen, M. Kowalczyk, *Slow Dynamics of Interior Spikes in the Shadow Gierer-Meinhardt System*, Adv. in Diff. Equat., **6**, No. 7, (2001), pp. 847–872.
- [6] X. Chen, M. Kowalczyk, *Dynamics of an Interior Spike in the Gierer-Meinhardt System*, SIAM J. Math. Anal., **33**, No. 1, (2001), pp. 172–193.
- [7] M. Del Pino, P. Felmer, M. Kowalczyk, *Boundary Spikes in the Gierer-Meinhardt System*, Commun. Pure Appl. Anal., **1**, No. 4, (2002), pp. 437–456.
- [8] A. Gierer, H. Meinhardt, *A Theory of Biological Pattern Formation*, Kybernetik, **12**, (1972), pp. 30–39.
- [9] C. Gui, J. Wei, *Multiple Interior Peak Solutions for Some Singularly Perturbed Neumann Problems*, J. Diff. Eq., **158**, No. 1, (1999), pp. 1–27.
- [10] B. Gustafsson, *On the Convexity of a Solution of Liouville's Equation*, Duke Math. J., **60**, No. 2, (1990), pp. 303–311.
- [11] L. Harrison, D. Holloway, *Order and Localization in Reaction-Diffusion Pattern*, Physica A, **222**, (1995), pp. 210–233.
- [12] D. Iron, M. J. Ward, *A Metastable Spike Solution for a Non-Local Reaction-Diffusion Model*, SIAM J. Appl. Math., **60**, No. 3, (2000), pp. 778–802.
- [13] D. Iron, M. J. Ward, *The Dynamics of Boundary Spikes for a Non-local Reaction-Diffusion Model*, Europ. J. Appl. Math., **11**, No. 5, (2000), pp. 491–514.
- [14] D. Iron, M. J. Ward, J. Wei, *The Stability of Spike Solutions to the One-Dimensional Gierer-Meinhardt Model*, Physica D, **150**, No. 1-2, (2001), pp. 25–62.
- [15] T. Kolokolnikov, M. J. Ward, *Reduced Wave Green's Functions and Their Effect on the Dynamics of a Spike for the Gierer-Meinhardt Model*, to appear, Europ. J. Appl. Math., (2003).
- [16] M. Kowalczyk, *Multiple Spike Layers in the Shadow Gierer-Meinhardt System: Existence of Equilibria and Approximate Invariant Manifold*, Duke Math. J., **98**, No. 1, (1999), pp. 59–111.
- [17] H. Meinhardt, *Models of Biological Pattern Formation*, Academic Press, London, (1982).
- [18] H. Meinhardt, *The Algorithmic Beauty of Sea Shells*, Springer-Verlag, Berlin, (1995).
- [19] W. Ni, *Diffusion, Cross-Diffusion, and Their Spike-Layer Steady-States*, Notices of the AMS, Vol. **45**, No. 1, (1998), pp. 9–18.
- [20] J. E. Pearson, *Complex Patterns in a Simple System*, Science, **216**, (1993), pp. 189–192.
- [21] Y. Nishiura, D. Ueyama, *A Skeleton Structure of Self-Replicating Dynamics*, Physica D, **130**, (1999), pp. 73–104.
- [22] M. J. Ward, *An Asymptotic Analysis of Localized Solutions for Some Reaction-Diffusion Models in Multi-Dimensional Domains*, Stud. Appl. Math., **97**, No. 2, (1996), pp. 103–126.
- [23] M. J. Ward, D. McNerney, P. Houston, D. Gavaghan, P. Maini, *The Dynamics and Pinning of a Spike for a Reaction-Diffusion System*, SIAM J. Appl. Math., **62**, No. 4, (2002), pp. 1297–1328.
- [24] J. Wei, *On Single Interior Spike Solutions for the Gierer-Meinhardt System: Uniqueness and Stability Estimates*, Europ. J. Appl. Math., **10**, No. 4, (1999), pp. 353–378.
- [25] J. Wei, *On the Boundary Spike Layer Solutions of Singularly Perturbed Semilinear Neumann Problem*, J. Diff. Eq., **134**, No. 1, (1997), pp. 104–133.
- [26] J. Wei, *On the Interior Spike Layer Solutions to a Singularly Perturbed Neumann Problem*, Tohoku Math. J., **50**, No. 2, (1998), pp. 159–178.
- [27] J. Wei, *Uniqueness and Critical Spectrum of Boundary Spike Solutions*, Proc. Royal Soc. Edinburgh, Section A (Mathematics), **131**, No. 6, (2001), pp. 1457–1480.
- [28] J. Wei, M. Winter, *Spikes for the Gierer-Meinhardt System in Two Dimensions: The Strong Coupling Case*, J. Diff. Eq., **178**, No. 2, (2002), pp. 478–518.
- [29] R. Wong, *Asymptotic Approximations of Integrals*, Academic Press, San Diego, CA, (1989).

Received March 2003; revised August 2003; final version January 2004.

E-mail address: tkolokol@math.ubc.ca

E-mail address: ward@math.ubc.ca